



SAPIENZA  
UNIVERSITÀ DI ROMA

**Nano** Rome, 15-18 September  
**2020 Innovation**  
Conference & Exhibition

**Design and synthesis of Quinolinonyl DKA derivatives as HIV-1 integrase inhibitors and nanotubes conjugation to improve their cell penetration.**

Dr.ssa Antonella Messori

# AIDS

Acquired Immunodeficiency Syndrome (AIDS) is a disease of the human immune system caused by Human Immunodeficiency Virus (HIV).

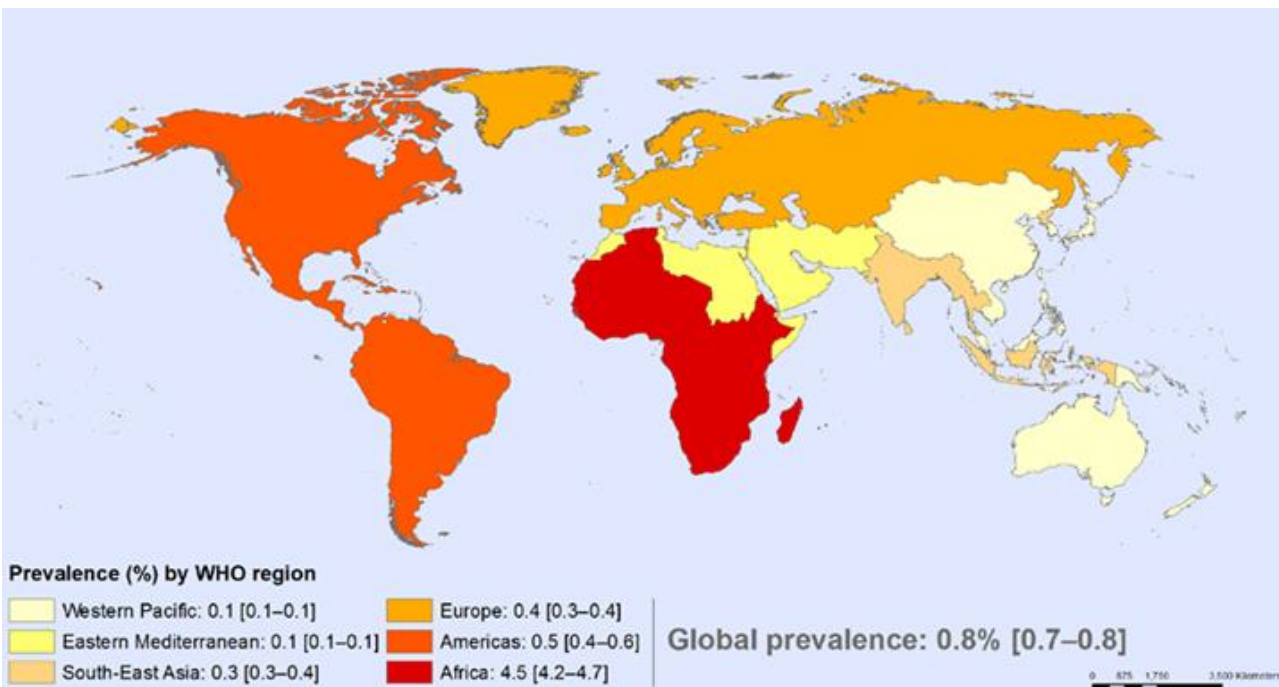


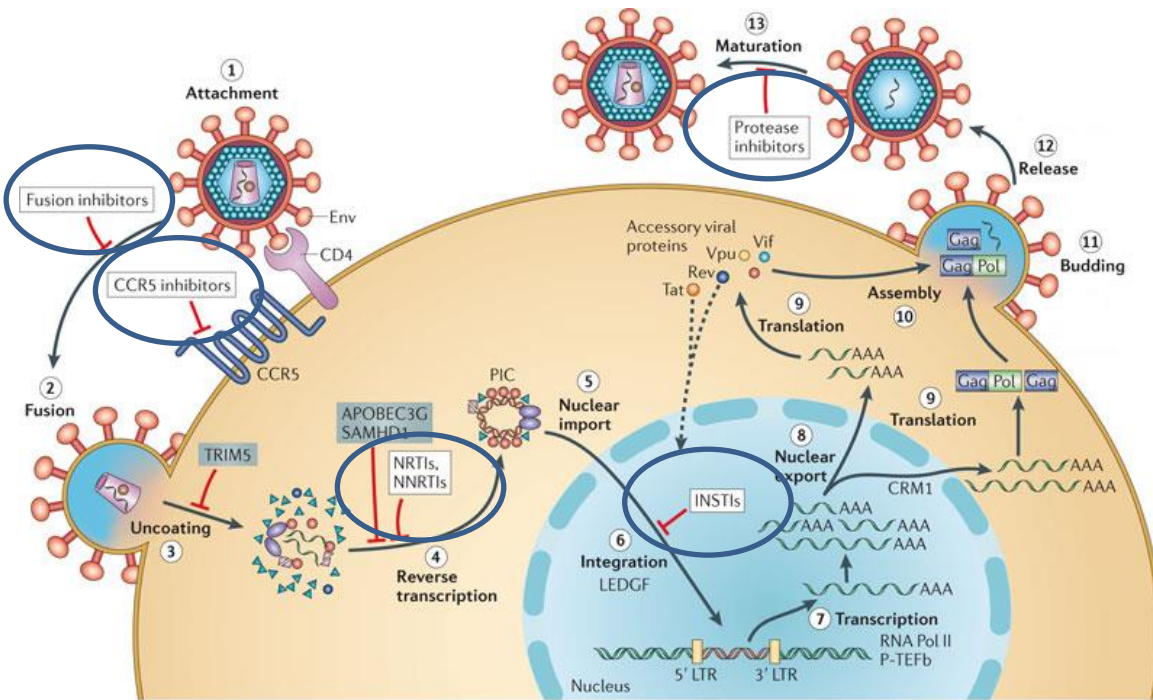
**Figure.** Global situation and trends: Since the beginning of the epidemic, almost 78 million people have been infected with the HIV virus. An estimated 0.8% of adults aged 15–49 years worldwide are living with HIV, although the burden of the epidemic continues to vary considerably between countries and regions.

## People living with HIV

- In 2019, there were 38.0 million [31.6 million–44.5 million] people living with HIV.
  - 36.2 million [30.2 million–42.5 million] adults.
  - 1.8 million [1.3 million–2.2 million] children (0–14 years).
- 81% [68–95%] of all people living with HIV knew their HIV status.
- About 7.1 million people did not know that they were living with HIV.



# Antiretroviral Therapy (ART)



Nature Reviews | Microbiology

Nat Rev Microbiol. 2012, 4, 279-290

- **Attachment Inhibitors (AI)**  
Fostemsavir (Rukobia )
- **Post-Attachment Inhibitors (PAI)**  
Ibalizumab-uiyk (Trogarzo)
- **Fusion Inhibitor**  
Enfuvirtide (Fuzeon).
- **CCR5 Inhibitor**  
Maraviroc (Selzentry).
- **Nucleoside RT Inhibitors (NRTIs)**  
Zidovudine (Retrovir), Didanosine (Videx)  
Zalcitabine (Hivid), Lamivudine (Epivir), Stavudine (Zerit), Abacavir (Ziagen), Emtricitabine (Emtriva), Tenofovir Disoproxil Fumarate (Viread).
- **Non-nucleoside RT Inhibitors (NNRTIs)**  
Nevirapine (Viramune), Delavirdine (Rescriptor), Efavirenz (Sustiva), Etravirine (Intence), Rilpivirine ( Edurant).
- **Integrase Inhibitors (INIs)**  
Raltegravir (Isentress), Elvitegravir (Vitekta), Dolutegravir (Tivicay)
- **Protease Inhibitors (PRIs)**  
Atazanavir (Reyataz), Saquinavir (Invirase), Ritonavir (Norvir), Darunavir (Prezista), Indinavir (Crixivan), Nelfinavir (Viracept), Fosamprenavir (Lexiva), Amprenavir (Agenerase), Lopinavir/Ritonavir (Kaletra), Tipranavir (Aptivus)
- **Pharmacokinetic Enhancers (PE)**  
Cobicistat (Tybast)

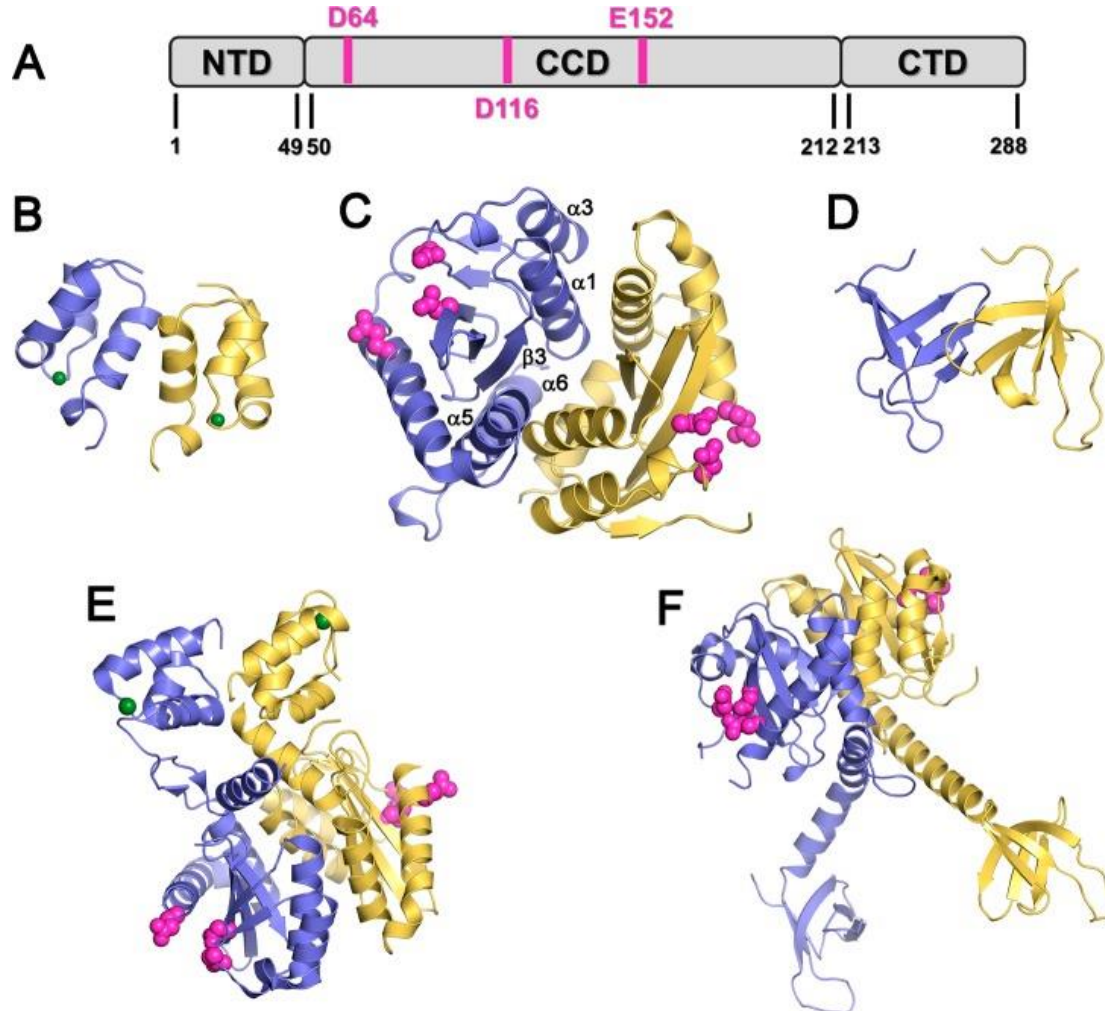
Limits of ART:  
**Development of new antiretrovirals is constantly needed!**  
 ✓ emergence of extensively cross-resistant strains of HIV-1  
 ✓ adverse effects of long-term use of these drug regimens



# HIV-1 Integrase (IN)

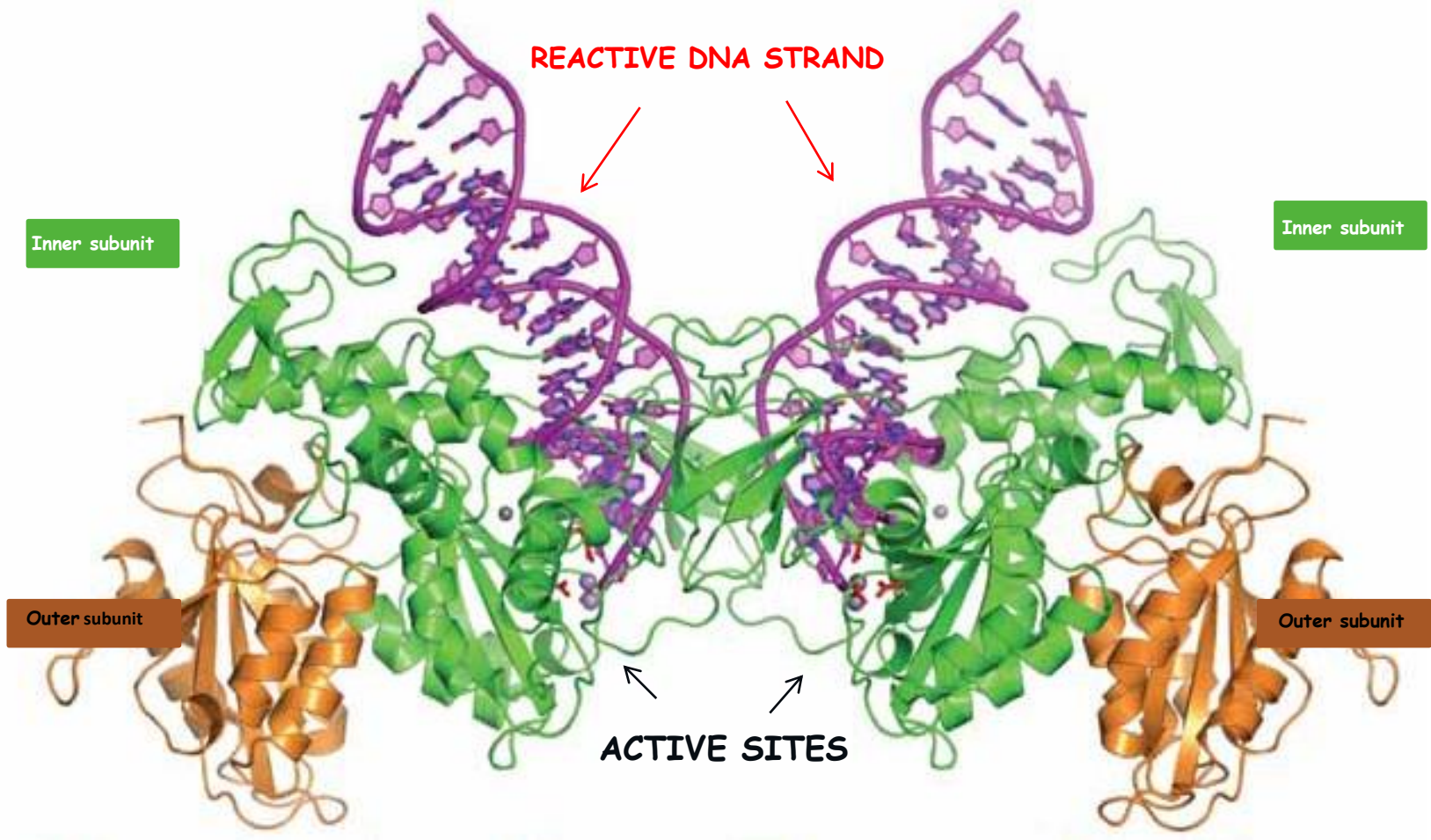
IN is a 32 kDa protein comprising three structural domains:

- N-terminal domain (NTD)
- catalytic core domain (CCD)
- C-terminal nonspecific DNA-binding domain (CTD).



Structure of HIV-1 IN. (A) IN domains, where the catalytic triad is shown in pink. (B-D) Structures of single IN domains: (B) NTD (PDB code 1wje); (C) CCD (PDB code 1bis); (D) CTD (PDB code 1ihv). (E-F) IN two-domain structures: (E) NTD + CCD (PDB code 1k6y); (F) CTD + CCD (PDB code 1ex4). Each structure consists of two IN monomers, shown in yellow and blue. The zinc ions in the NTD are shown in green, and the catalytic triad (D64, D116, and E152) in the CCD is shown in pink.

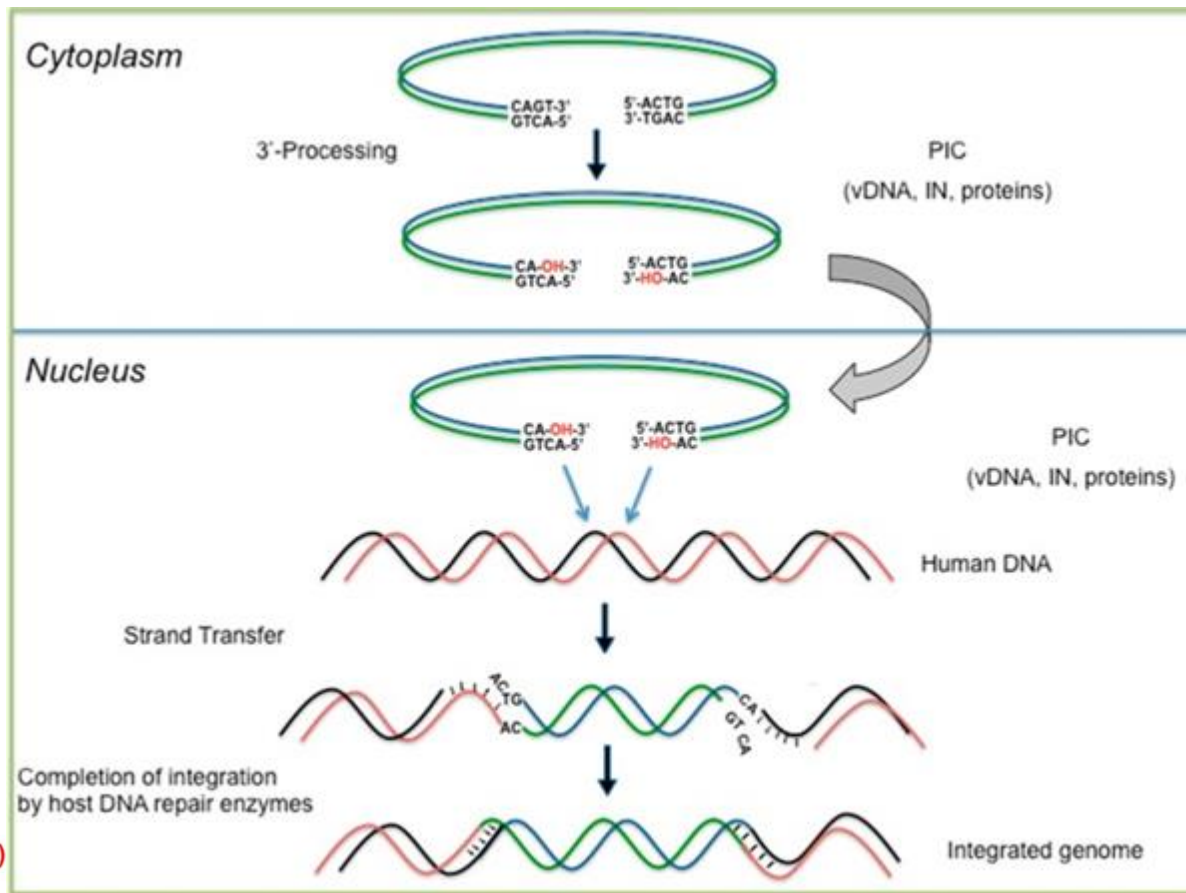
# Integrase



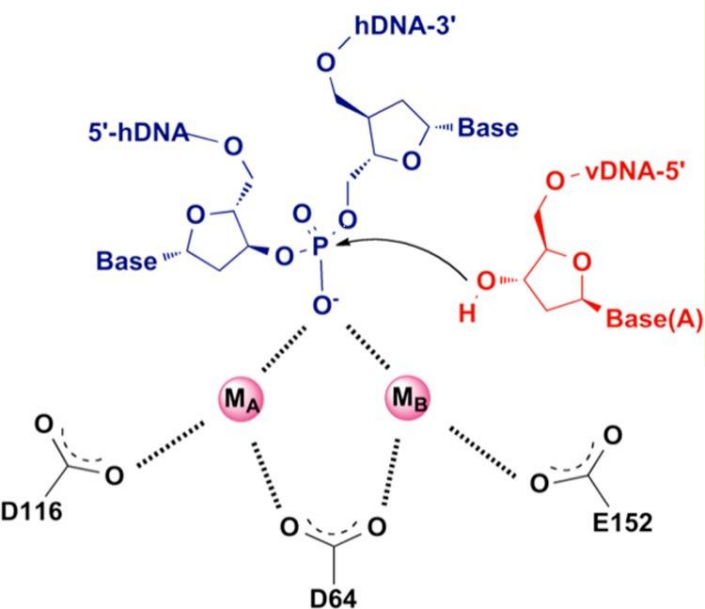
Architecture of the PFV intasome.

# Integrase: Mechanism of catalysis

- 3'- Processing (3'-P)
- Strand Transfer (ST)



Outline of the in vivo integration process

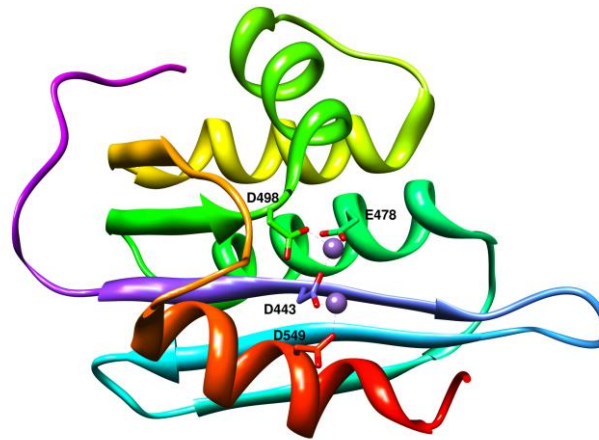


ST step. The attack of the 3' ends of vDNA on the phosphodiester bonds of host DNA is coordinated by metal ions.

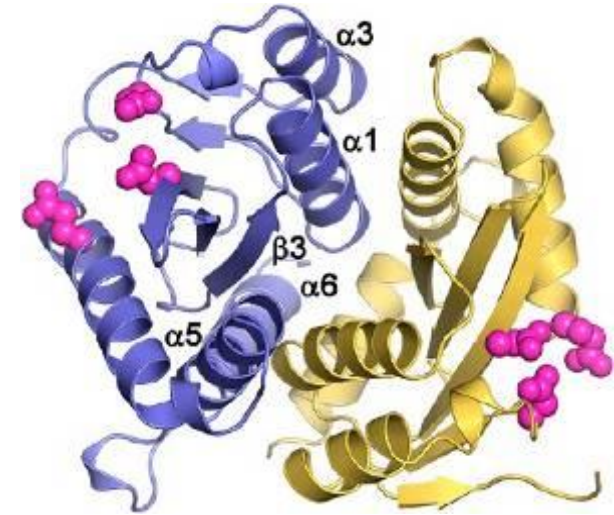
*J. Med Chem.* **2014**, *3*, 539-566.

# Similarities and differences: IN and RNase H

**STRUCTURAL  
SIMILARITIES**

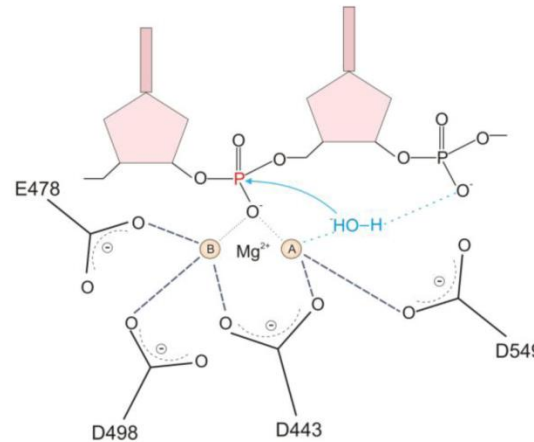


**RNase H active site**

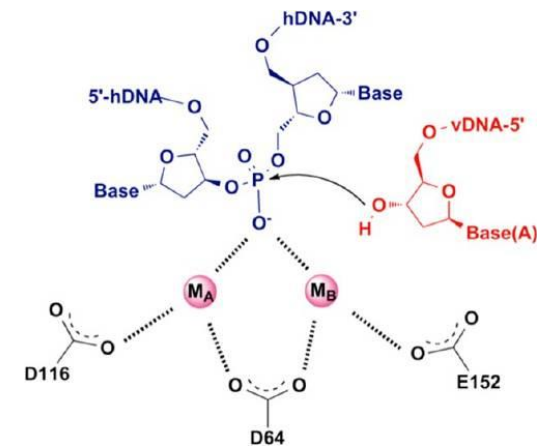


**IN active site**

**DIFFERENCES IN THE  
CATALYTIC  
MECHANISM**

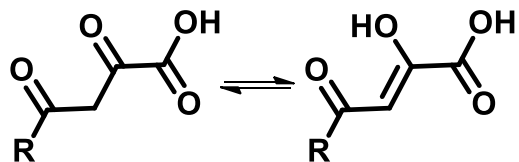


Biology 2012, 1(3), 521-541



Mol. Cell 2006, 22, 5-13.

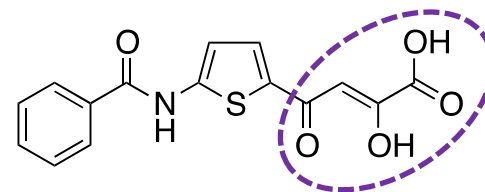
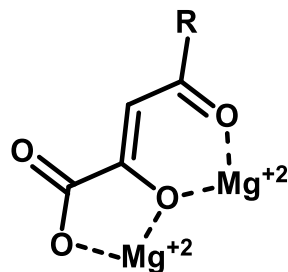
# Dual RNase H function and Integrase inhibitors.



$\alpha,\gamma$ diketo acid (DKA) group

*J. Med. Chem.* **2008**, *51*(15), 4744-4750.

*J. Med. Chem.* **2006**, *49*(6), 1939-1945.

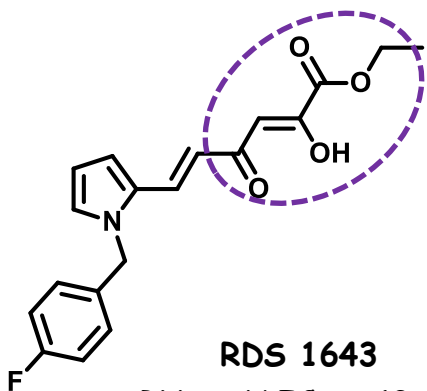


**BTDBA**

RNase H  $IC_{50}$  = 3.2  $\mu$ M

IN (ST)  $IC_{50}$  = 1.9  $\mu$ M

*J. Biol. Chem.* **2003**, *278*, 2777-2780.

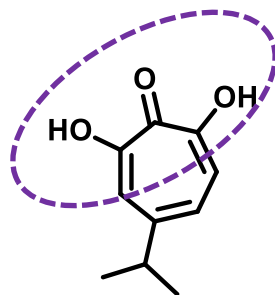


**RDS 1643**

RNase H  $IC_{50}$  = 13  $\mu$ M

IN (ST)  $IC_{50}$  = 98  $\mu$ M

*Antiviral Res.* **2005**, *65*, 117-124

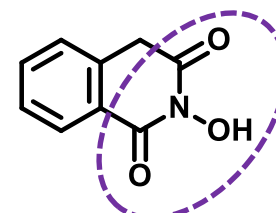


$\beta$ -Thujaplicinol

RNase H  $IC_{50}$  = 0,2  $\mu$ M

IN (ST)  $IC_{50}$  = 21  $\mu$ M

*Antimicrob. Agents Chemother.* **2005**, *49*, 4884-4894



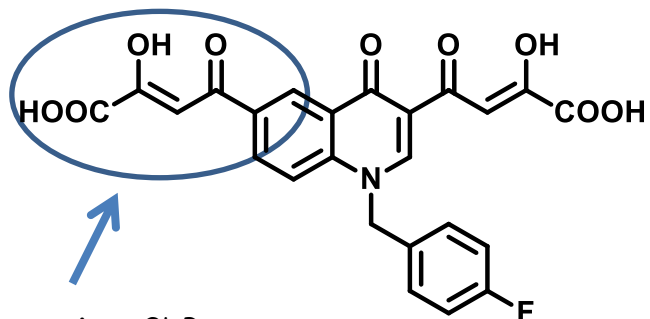
2-hydroxyquinoline-1,3(2H,4H)dione

RNase H  $IC_{50}$  = 1  $\mu$ M

IN (ST)  $IC_{50}$  = 6,32  $\mu$ M

*Nucleic Acids Res.* **2003**, *31*, 6852-6859.

# Aim 1

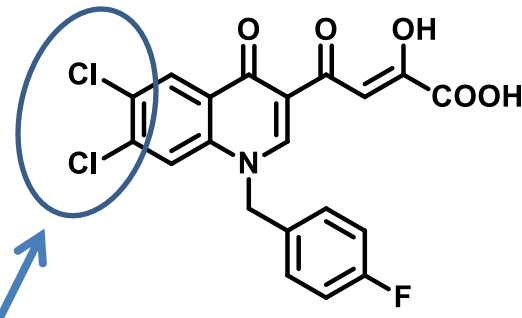


Activity against 3'-P

RDS 1997 (1)

$IC_{50}$  3'-P = 200 nM  
 $IC_{50}$  ST = 12 nM

*J. Med. Chem.* 2006, 49, 1939-194.

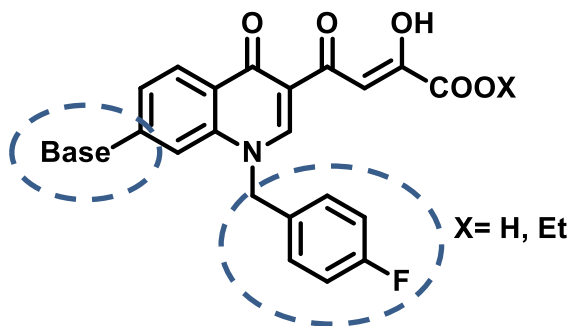


Selective against ST

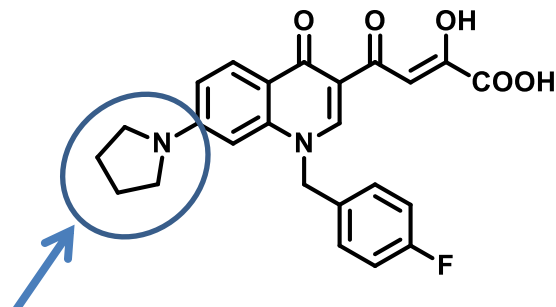
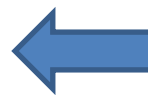
RDS 2188 (2)

$IC_{50}$  3'-P > 50  $\mu$ M  
 $IC_{50}$  ST = 33 nM

*J. Med. Chem.* 2008, 51, 4744-4750.



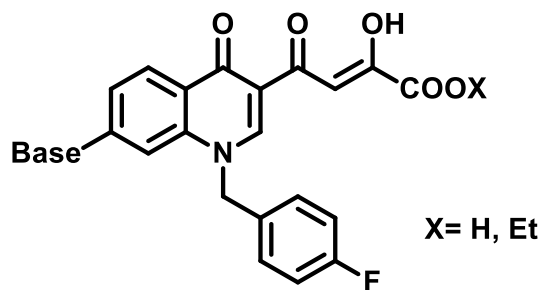
4a-e,g,h and 5a-e,g,h



Activity against IN and RNase H RDS 2197 (3b)

$IC_{50}$  3'-P = 14.9  $\mu$ M  
 $IC_{50}$  ST = 28 nM  
 $IC_{50}$  RNase H = 5.1  $\mu$ M

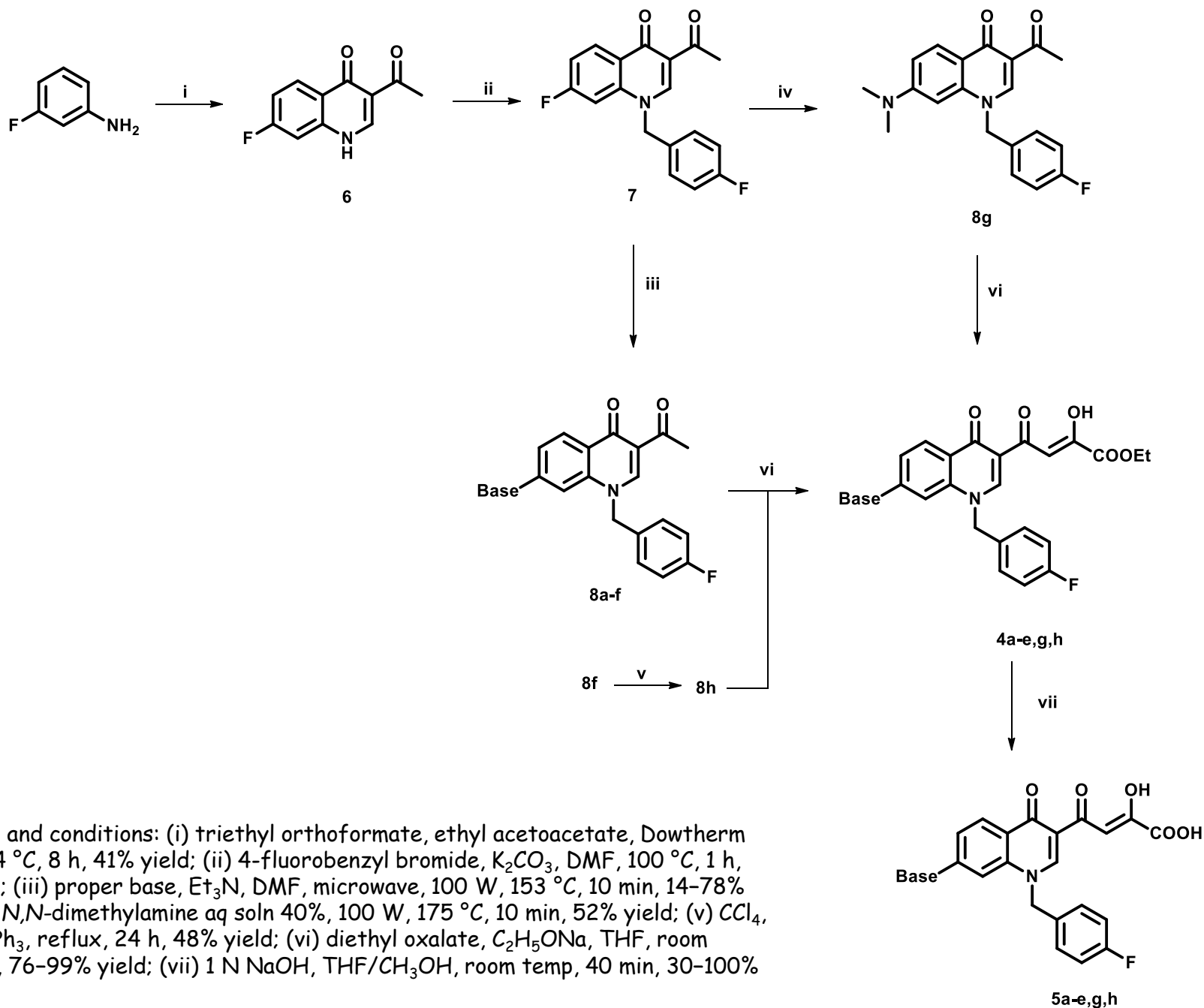
# Basic Quinolinonyl DKA derivatives



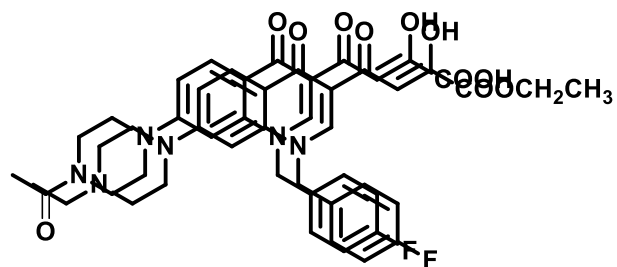
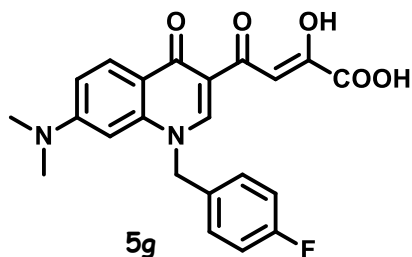
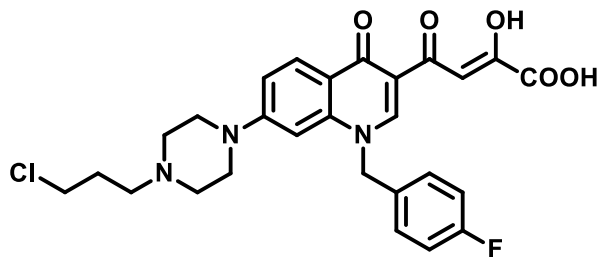
4a-e,g,h and 5a-e,g,h

Cpd	Base	X
4a		Et
4b		Et
4c		Et
4d		Et
4e		Et
4g		Et
4h		Et
5a		H
5b		H
5c		H
5d		H
5e		H
5g		H
5h		H

# Scheme 1. Synthetic Route to Quinolinonyl DKAs **4a-e,g,h** and **5a-e,g,h**.<sup>a</sup>



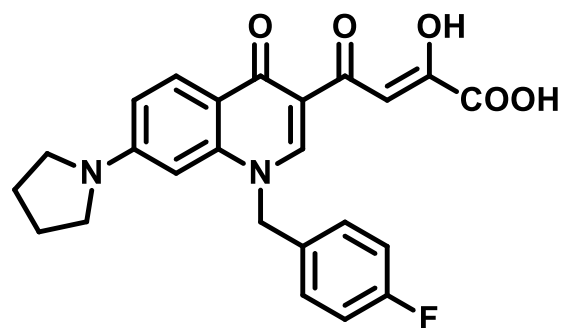
<sup>a</sup>Reagents and conditions: (i) triethyl orthoformate, ethyl acetoacetate, Dowtherm A, 95–254 °C, 8 h, 41% yield; (ii) 4-fluorobenzyl bromide,  $K_2CO_3$ , DMF, 100 °C, 1 h, 29% yield; (iii) proper base,  $Et_3N$ , DMF, microwave, 100 W, 153 °C, 10 min, 14–78% yield; (iv) *N,N*-dimethylamine aq soln 40%, 100 W, 175 °C, 10 min, 52% yield; (v)  $CCl_4$ ,  $CH_2Cl_2$ ,  $PPh_3$ , reflux, 24 h, 48% yield; (vi) diethyl oxalate,  $C_2H_5ONa$ , THF, room temp, 2 h, 76–99% yield; (vii) 1 N NaOH, THF/ $CH_3OH$ , room temp, 40 min, 30–100% yield.

**Table 1.** Cytotoxicity, Antiviral, Anti-IN, anti-RNase H Activities ofCompounds **4a-e,g,h** and **5a-e,g,h****4c**  
**5d****5g****5h**

Cpd	Base	X	enzymatic activity			antiviral activity			
			IN IC <sub>50</sub> <sup>a</sup> (μM)	3'-P <sup>c</sup>	% in. at 10 μM <sup>d</sup>	RNase H IC <sub>50</sub> <sup>e</sup> (μM)	EC <sub>50</sub> <sup>f</sup>	CC <sub>50</sub> <sup>g</sup>	SI <sup>h</sup>
4a	—N—NH	Et	24 ± 1	>333	18	nd <sup>i</sup>	20.9	>50	>2.4
4b	—N—N-CH <sub>3</sub>	Et	0.6 ± 0.1	56 ± 8	41	18.5 ± 0.7	33.1	nt	nt
4c	—N—N-C <sub>2</sub> H <sub>5</sub>	Et	2.4 ± 0.3	>111	63	26.2 ± 0.9	3.6	>50	>13.8
4d	—N—N-C(=O)CH <sub>3</sub>	Et	0.17 ± 0.04	17 ± 1	30	nd	>50	nd	nd
4e	—N—O	Et	2.1 ± 0.2	>111	0.7	nd	16.2	>50	>3.0
4g	—N(CH <sub>3</sub> ) <sub>2</sub>	Et	2.9 ± 0.4	41 ± 2	26	nd	>50	nd	nd
4h	—N—N-CH <sub>2</sub> CH <sub>2</sub> CH <sub>2</sub> Cl	Et	1.3 ± 0.3	102 ± 17	35	nd	13.2	>50	>3.7
5a	—N—NH	H	2.0 ± 0.3	65 ± 2	44	28.7 ± 0.7	>50	nd	nd
5b	—N—N-CH <sub>3</sub>	H	0.10 ± 0.01	8.5 ± 0.9	34	nd	>50	nd	nd
5c	—N—N-C <sub>2</sub> H <sub>5</sub>	H	0.21 ± 0.06	23 ± 2	22	nd	>50	nd	nd
5d	—N—N-C(=O)CH <sub>3</sub>	H	0.08 ± 0.01	8.5 ± 0.7	74	3.3 ± 0.1	17	>50	>2.9
5e	—N—O	H	0.08 ± 0.1	13 ± 1	72	6.8 ± 0.1	26.3	>50	>1.9
5g	—N(CH <sub>3</sub> ) <sub>2</sub>	H	0.15 ± 0.02	5.1 ± 0.5	66	6.6 ± 0.3	>50	nd	nd
5h	—N—N-CH <sub>2</sub> CH <sub>2</sub> CH <sub>2</sub> Cl	H	0.05 ± 0.01	4.6 ± 0.5	78	5.7 ± 0.1	>50	nd	nd
3a <sup>j</sup>	—N—	Et	2.3	110	55.6	nd	0.83	>50	>60
63b <sup>j</sup>	—N—	H	0.028	14.9	71	5.1 ± 0.2	14.1	>50	>3.5
EVG			0.028±0.006 <sup>k</sup>	8.1±4.2 <sup>k</sup>	nd	91±8	0.0142±0.0052	>50	>3521
RAL			0.087±0.008 <sup>j</sup>	12.8±6 <sup>k</sup>	nd	100	0.0236±0.0046	>50	>2118

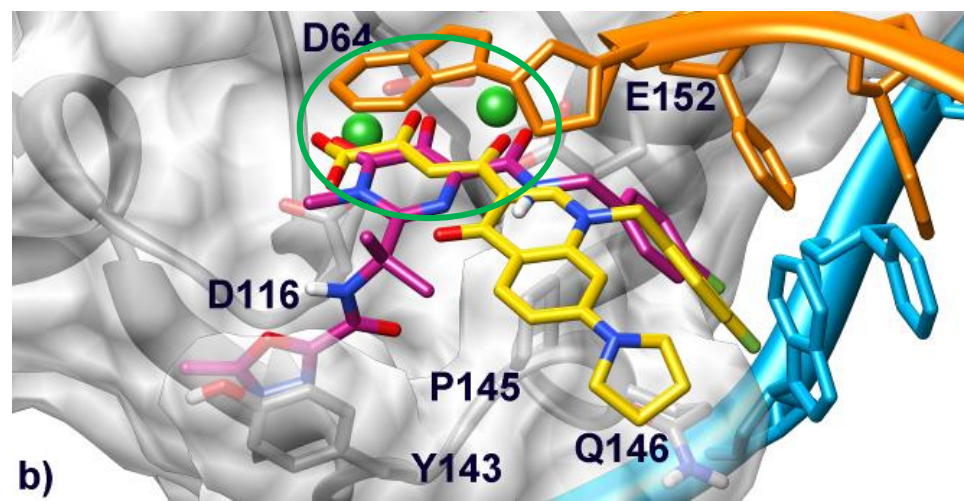
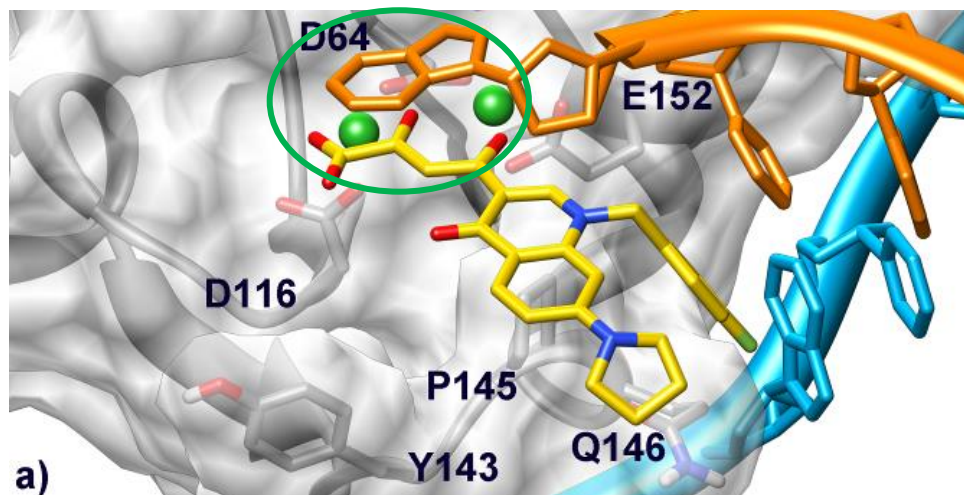
<sup>a</sup>Inhibitory concentration 50% (μM) determined against rIN from gel-based assays and expressed as mean ± SD from at least three independent experiments. <sup>b</sup>ST: strand transfer. <sup>c</sup>3'-P: 3'-processing. <sup>d</sup>Percentage of inhibition of RT-associated RNase H activity at fixed concentration of inhibitor 10 μM (%). <sup>e</sup>Inhibitory concentration 50% against HIV-1 RT-associated RNase H activity determined from dose response curves (μM). <sup>f</sup>Effective concentration 50% in HIV-1 infected HeLa cells (μM). <sup>g</sup>Cytotoxic concentration 50% in HeLa cells (μM). <sup>h</sup>Selectivity index (CC<sub>50</sub>/EC<sub>50</sub>). <sup>i</sup>nd: not determined. <sup>j</sup>Reference 151. <sup>k</sup>Reference 155.

# Binding Mode of 3b within HIV-1 IN/DNA model.



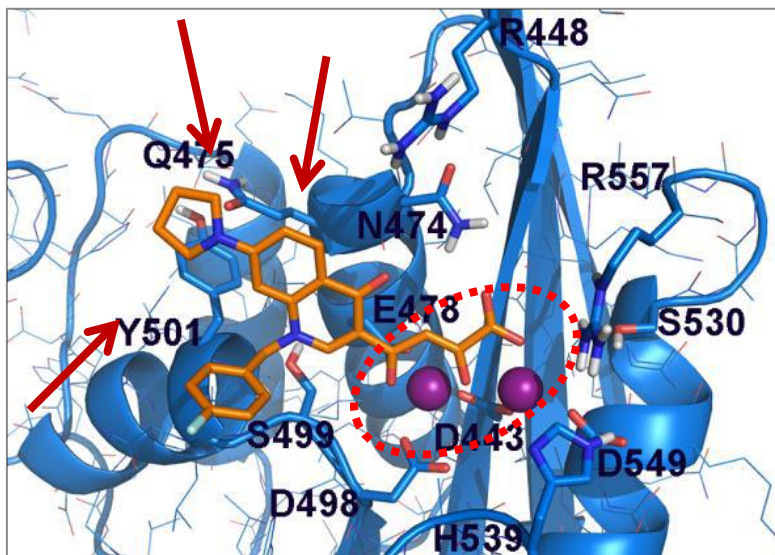
3b

Cmpd	IN IC <sub>50</sub> (μM)		RNase-H IC <sub>50</sub> (%)	
	ST	3'-P	(μM)	in. at 10 μM
3b	0.028	14.9	5.1	71

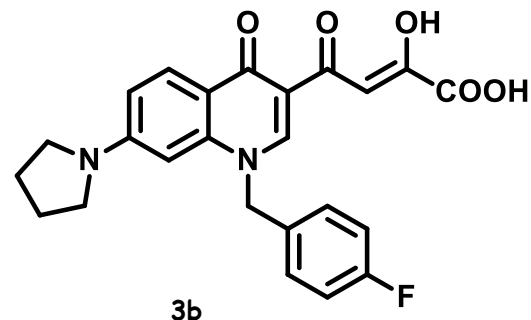


**Figure.** a) Binding mode of compound 3b (yellow) within the HIV-1 IN/DNA model. Catalytic core domain is depicted as transparent light gray surface and ribbons. Amino acid side chains involved in ligand binding are represented as sticks. The non-cleaved (cyan) and processed (orange) viral DNA strands are shown as ribbon and sticks. Mg<sup>2+</sup> metal ions are represented as green spheres. b) Overlay of compound 3b and Raltegravir (magenta) in the IN binding pocket.

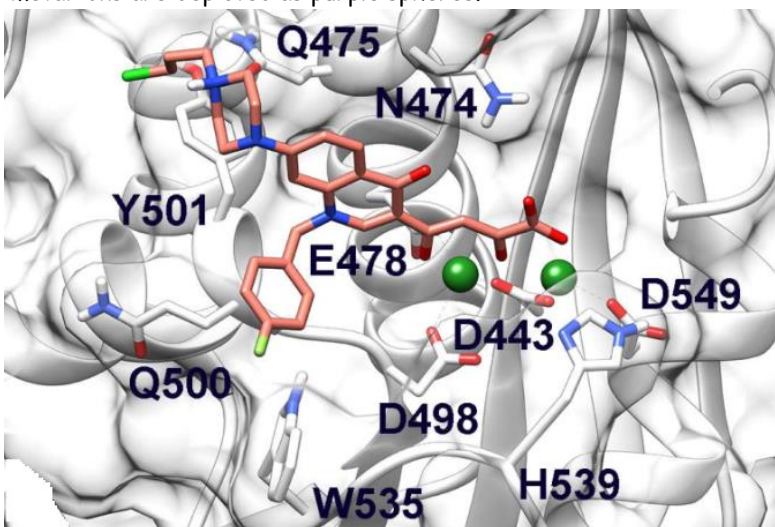
# Binding mode of 3b in the HIV-1 RNase H active site.



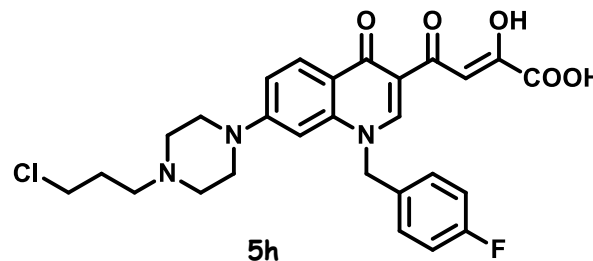
**Figure.** Binding mode of compound 3b (orange) in the HIV-1 RNase H active site. Amino acid side chains important for ligand binding are represented as sticks. Mg<sup>2+</sup> metal ions are depicted as purple spheres.



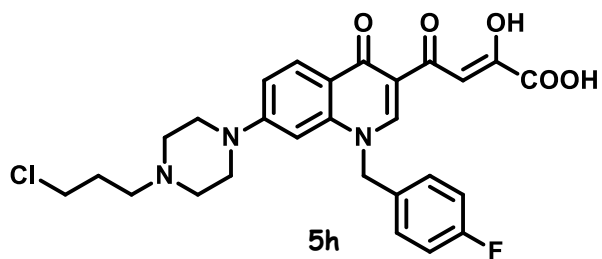
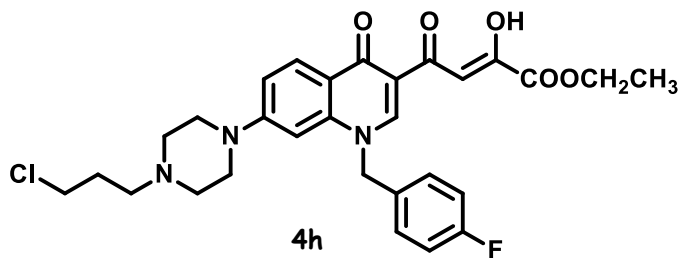
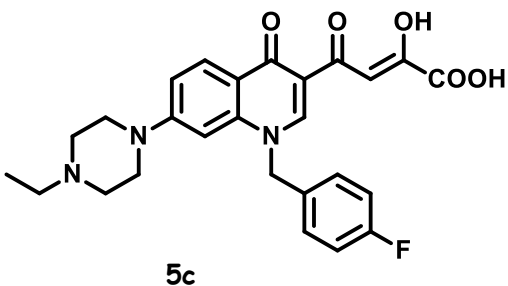
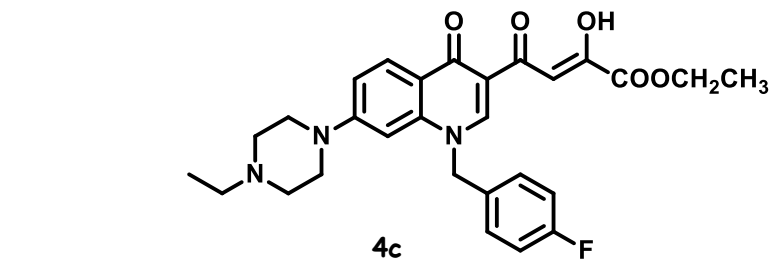
Cmpd	IN IC <sub>50</sub> (μM)		RNase-H IC <sub>50</sub> (μM) % in. at 10 μM	
	ST	3'-P		
<b>3b</b>	0.028	14.9	5.1	71



**Figure.** Binding mode of compound 5h (pink sticks) in the HIV-1 RNase H active site.



Cmpd	IN IC <sub>50</sub> (μM)		RNase-H IC <sub>50</sub> (μM) % in. at 10 μM	
	ST	3'-P		
<b>5h</b>	0.05±0.01	4.6±0.5	5.7±0,1	78

**Table 1.** Cytotoxicity, Antiviral, Anti-IN, anti-RNase H Activities ofCompounds **4a-e,g,h** and **5a-e,g,h**

Cpd	Base	X	enzymatic activity			antiviral activity			
			IN IC <sub>50</sub> <sup>a</sup> (μM)	3'-P <sup>c</sup>	% in. at 10 μM <sup>d</sup>	RNase H IC <sub>50</sub> <sup>e</sup> (μM)	EC <sub>50</sub> <sup>f</sup>	CC <sub>50</sub> <sup>g</sup>	SI <sup>h</sup>
4a		Et	24 ± 1	>333	18	nd <sup>i</sup>	20.9	>50	>2.4
4b		Et	0.6 ± 0.1	56 ± 8	41	18.5 ± 0.7	33.1	nt	nt
4c		Et	2.4 ± 0.3	>111	63	26.2 ± 0.9	3.6	>50	>13.8
4d		Et	0.17 ± 0.04	17 ± 1	30	nd	>50	nd	nd
4e		Et	2.1 ± 0.2	>111	0.7	nd	16.2	>50	>3.0
4g		Et	2.9 ± 0.4	41 ± 2	26	nd	>50	nd	nd
4h		Et	1.3 ± 0.3	102 ± 17	35	nd	13.2	>50	>3.7
5a		H	2.0 ± 0.3	65 ± 2	44	28.7 ± 0.7	>50	nd	nd
5b		H	0.10 ± 0.01	8.5 ± 0.9	34	nd	>50	nd	nd
5c		H	0.21 ± 0.06	23 ± 2	22	nd	>50	nd	nd
5d		H	0.08 ± 0.01	8.5 ± 0.7	74	3.3 ± 0.1	17	>50	>2.9
5e		H	0.08 ± 0.1	13 ± 1	72	6.8 ± 0.1	26.3	>50	>1.9
5g		H	0.15 ± 0.02	5.1 ± 0.5	66	6.6 ± 0.3	>50	nd	nd
5h		H	0.05 ± 0.01	4.6 ± 0.5	78	5.7 ± 0.1	>50	nd	nd
3a <sup>j</sup>		Et	2.3	110	55.6	nd	0.83	>50	>60
3b <sup>j</sup>		H	0.028	14.9	71	5.1 ± 0.2	14.1	>50	>3.5
EVG			0.028±0.006 <sup>k</sup>	8.1±4.2 <sup>k</sup>	nd	91±8	0.0142±0.0052	>50	>3521
RAL			0.087±0.008 <sup>j</sup>	12.8±6 <sup>k</sup>	nd	100	0.0236±0.0046	>50	>2118

<sup>a</sup>Inhibitory concentration 50% (μM) determined against rIN from gel-based assays and expressed as mean ± SD from at least three independent experiments. <sup>b</sup>ST: strand transfer. <sup>c</sup>3'-P: 3'-processing. <sup>d</sup>Percentage of inhibition of RT-associated RNase H activity at fixed concentration of inhibitor 10 μM (%). <sup>e</sup>Inhibitory concentration 50% against HIV-1 RT-associated RNase H activity determined from dose response curves (μM). <sup>f</sup>Effective concentration 50% in HIV-1 infected HeLa cells (μM). <sup>g</sup>Cytotoxic concentration 50% in HeLa cells (μM). <sup>h</sup>Selectivity index (CC<sub>50</sub>/EC<sub>50</sub>). <sup>i</sup>nd: not determined.

# Aim 2

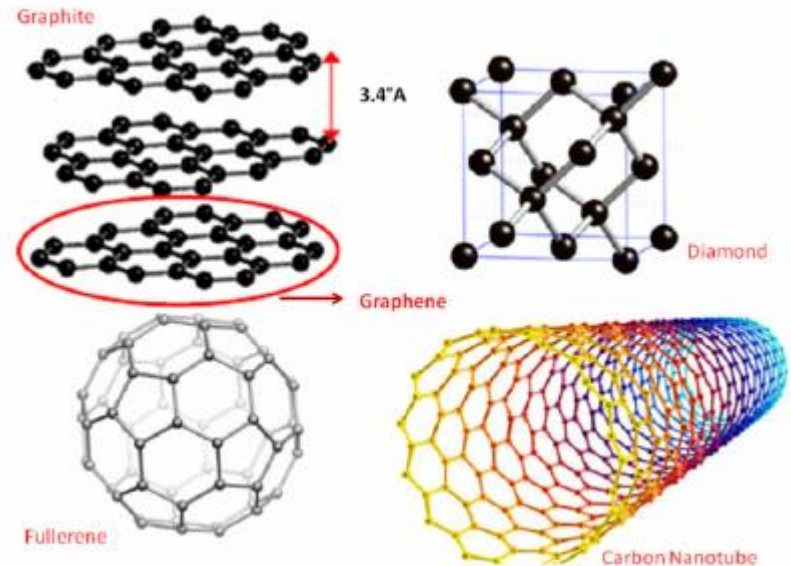
- DKAs limits**
- high metabolic turnover
  - poor membrane penetration



**lower *in vivo* activity**

Approaches to improve cell penetration:

- ❖ Carbon Nanotubes (CNTs) conjugation



# Carbon nanotubes (CNT)

CNTs can be defined as a graphene sheet rolled up to form a seamless cylinder made of  $sp^2$  hybridized carbon atoms.

- ✓ single-walled CNTs (SWCNTs)
- ✓ double-walled CNTs (DWCNTs)
- ✓ multi-walled CNTs (MWCNTs).

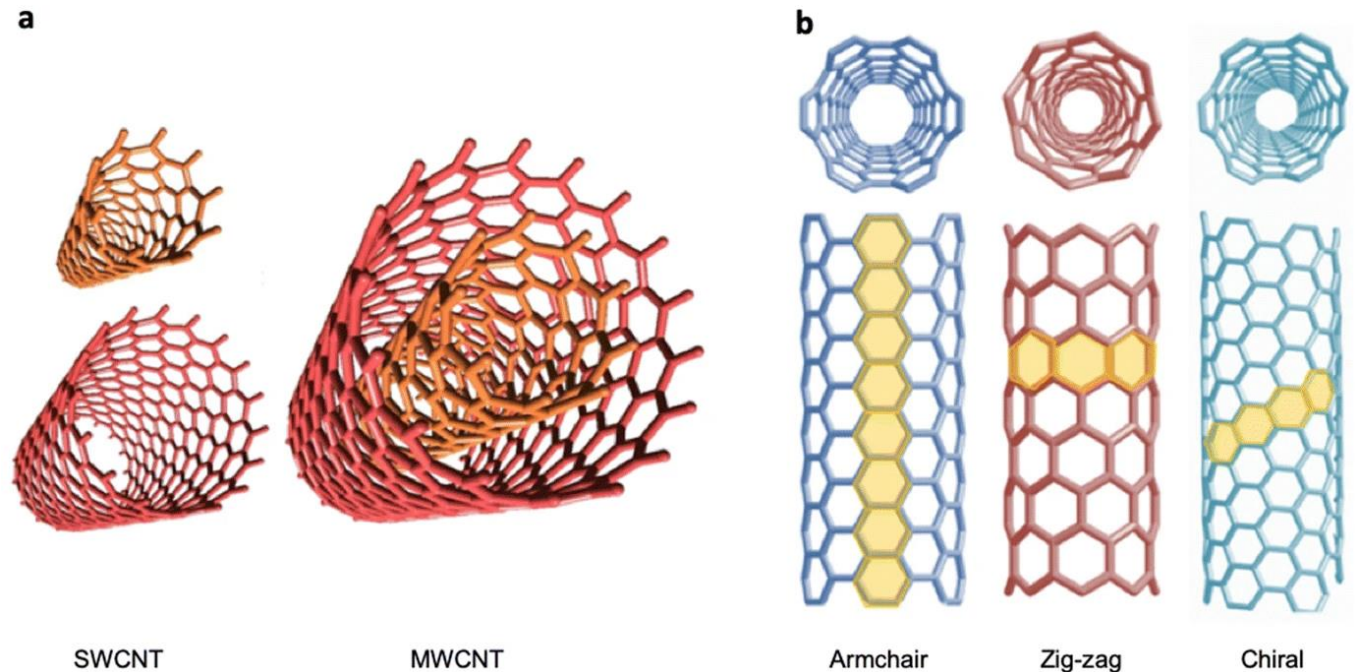


**Figure:** Carbon nanotube classifications. **a** According to the number of sheets, there are single- (SWCNTs) and multi-wall carbon nanotubes (MWCNTs); **b** depending on the rolling up of the sheets, they can be armchair, zig-zag, or chiral. *Top Curr Chem (Z)* **378**, 15 (2020). <https://doi.org/10.1007/s41061-019-0278-8>.

# Applications of CNTs

CNTs have emerged as a powerful tool to improve biomedical approaches in the management of numerous diseases. Nanotubes offer some advantages relative to nanoparticles by the following aspects:

1. Larger inner volumes - can be filled with chemical or biological species.
2. Nanotubes have the inner surface accessible.
3. Distinct inner and outer surface can be modified separately.

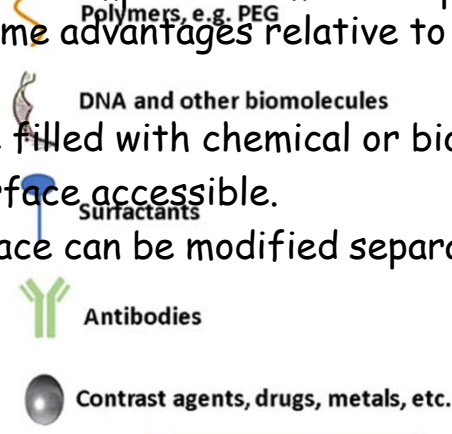
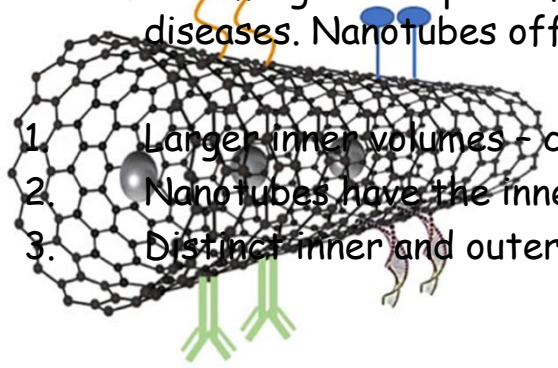


Figure. Schematic representation of surface functionalization and loading of carbon nanotubes for biomedical applications

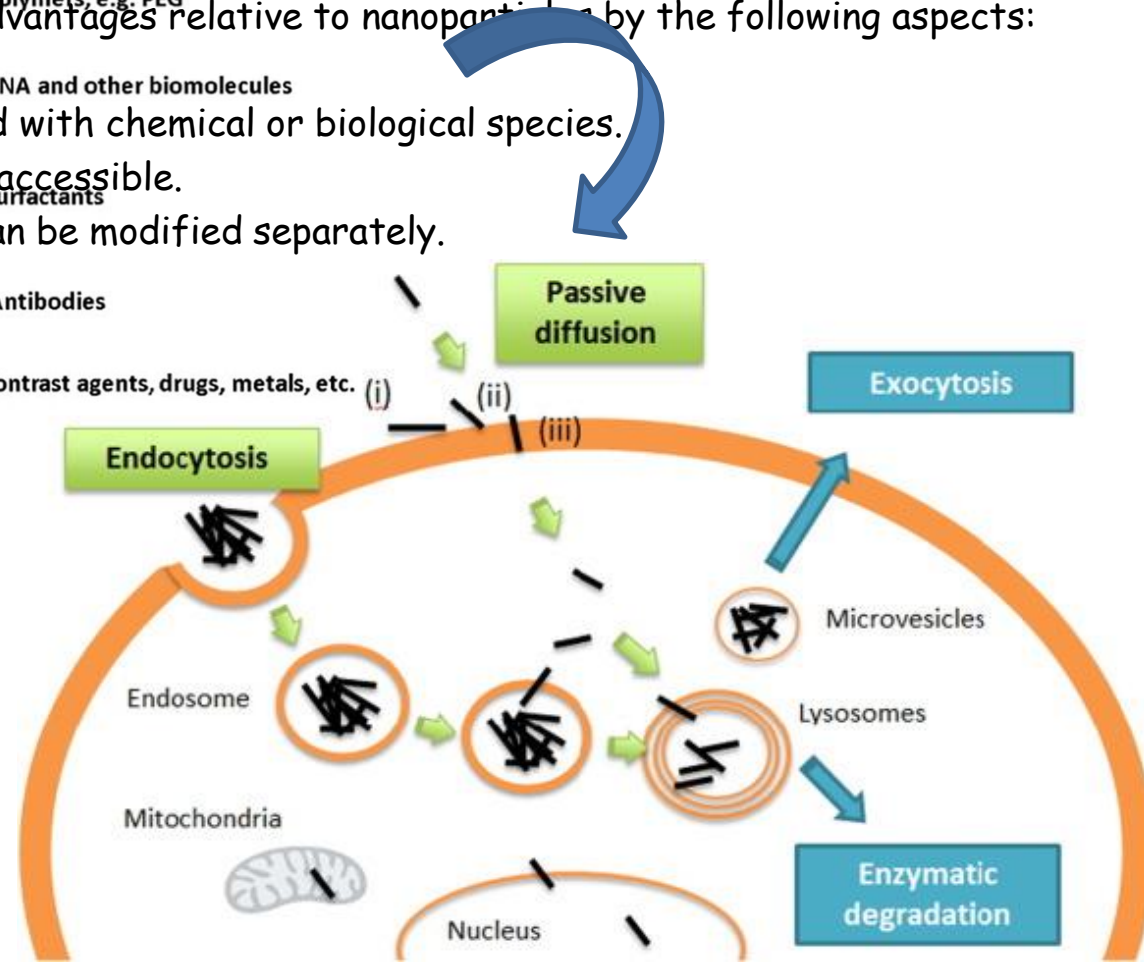
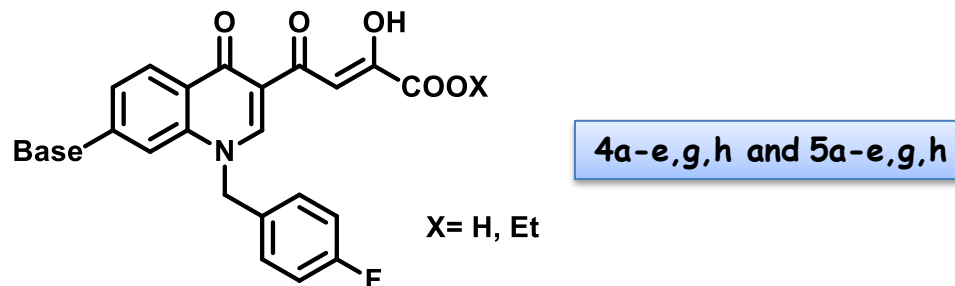


Figure. Uptake and cellular fate of f-CNTs in mammalian cells. The bundled MWNTs bind to cellular membranes and are then internalised into cells by endocytosis. In the endosomes, bundles release single MWNT, which penetrate through endosomal membranes and enter the cytosol. Alternatively, short and individualised CNTs (i) land on the surface of the plasma membrane, (ii) penetrate the lipid head groups and finally (iii) slide through the lipid tails to passively diffuse through the cell membrane. Both residual bundled MWNT in endosomes and free MWNT in the cytosol are recruited into lysosomes. CNTs can be excreted by exocytosis (not shown) or in autophagic microvesicles in case of cellular stress. Another exit mechanism has been reported in polynuclear neutrophils and macrophages where nanotubes are digested enzymatically. CNTs are also able to enter organelles and the nucleus.

# Conclusions

- Bifunctional quinolinonyl DKA derivatives were first described as nonselective inhibitors of 3'-processing (3'-P) and strand transfer (ST) functions of HIV-1 integrase (IN).
- Designed and synthesized a novel quinolinonyl diketo acid derivatives (**4a-e,g,h** and **5a-e,g,h**) endowed with a "base-like".



- Molecular modeling study on both the enzyme were performed
- Functionalized carbon nanotubes (MWCNTs)



SAPIENZA  
UNIVERSITÀ DI ROMA

# Acknowledgements

**Nano** Rome, 15-18 September  
**2020 Innovation**  
Conference & Exhibition



ISTITUTO PASTEUR  
FONDAZIONE CENCI BOLOGNETTI  
LA RICERCA IN PERSONA

DIPARTIMENTO DI CHIMICA  
E TECNOLOGIE DEL FARMACO

Chemistry

Roberto Di Santo, Roberta Costi,  
Valentina Noemi Madia, Luigi Scipione,  
Alessandro De Leo, Valeria Tudino

IN Enzyme and Cellular  
Assays

Yves Pommier  
Christophe Marchand  
Stuart Le Grice



INSTITUTE  
OF TROPICAL  
MEDICINE  
ANTWERP

Antiviral activity  
Guido Vanham



RNase H Enzyme Assays  
Enzo Tramontano



UNIVERSITÀ  
DEGLI STUDI DI TRIESTE

CNTs synthesis  
Maurizio Prato  
Tatiana Da Ros

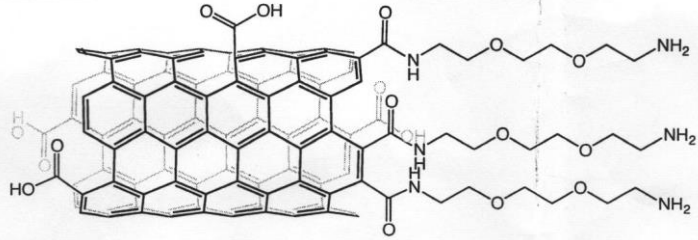


Molecular Modeling  
Sandro Cosconati  
Ettore Novellino



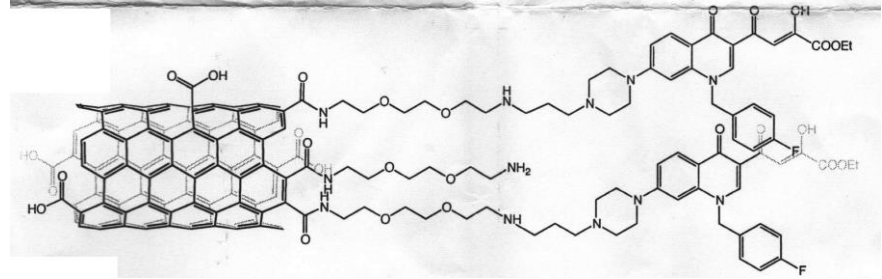
# Cell-penetrating CNTs for delivery of therapeutics

**LD-85**



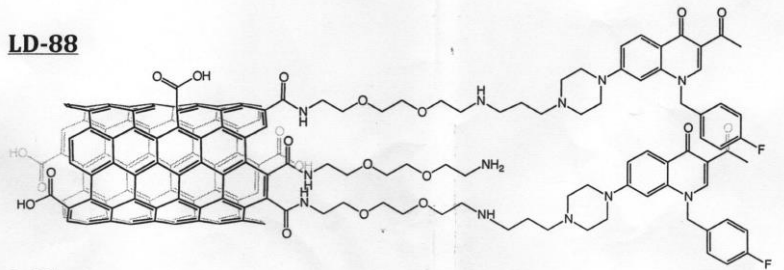
Loading (amino groups) = 137  $\mu\text{mol/g}$   
Dispersibility ( $\text{H}_2\text{O}$ )  $\approx 0.5$  mg/ml

**LD-97**



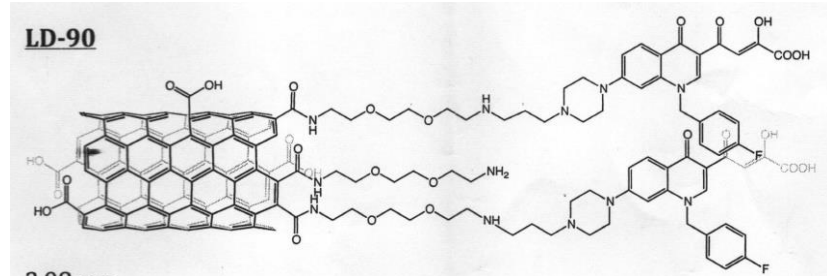
Loading (RDS 2832) = 105  $\mu\text{mol/g}$   
Dispersibility ( $\text{H}_2\text{O}$ )  $\approx 0.5$  mg/ml

**LD-88**



Loading (RDS 2831) = 35  $\mu\text{mol/g}$   
Dispersibility ( $\text{H}_2\text{O}$ )  $\approx 0.5$  mg/ml

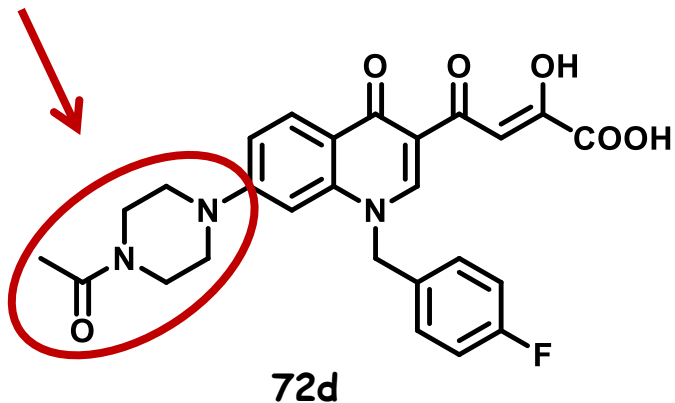
**LD-90**



Loading (RDS 2833) = 57  $\mu\text{mol/g}$   
Dispersibility ( $\text{H}_2\text{O}$ )  $\approx 0.5$  mg/ml

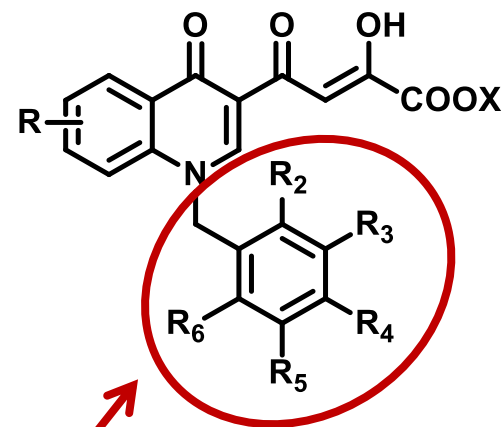
# Aim 2

Activity against IN and RNase H



$IC_{50}$  RNase H = 3.3  $\mu$ M  
 $IC_{50}$  IN ST = 80 nM

*J. Med. Chem.* 2014, 57(8), 3223-3234.

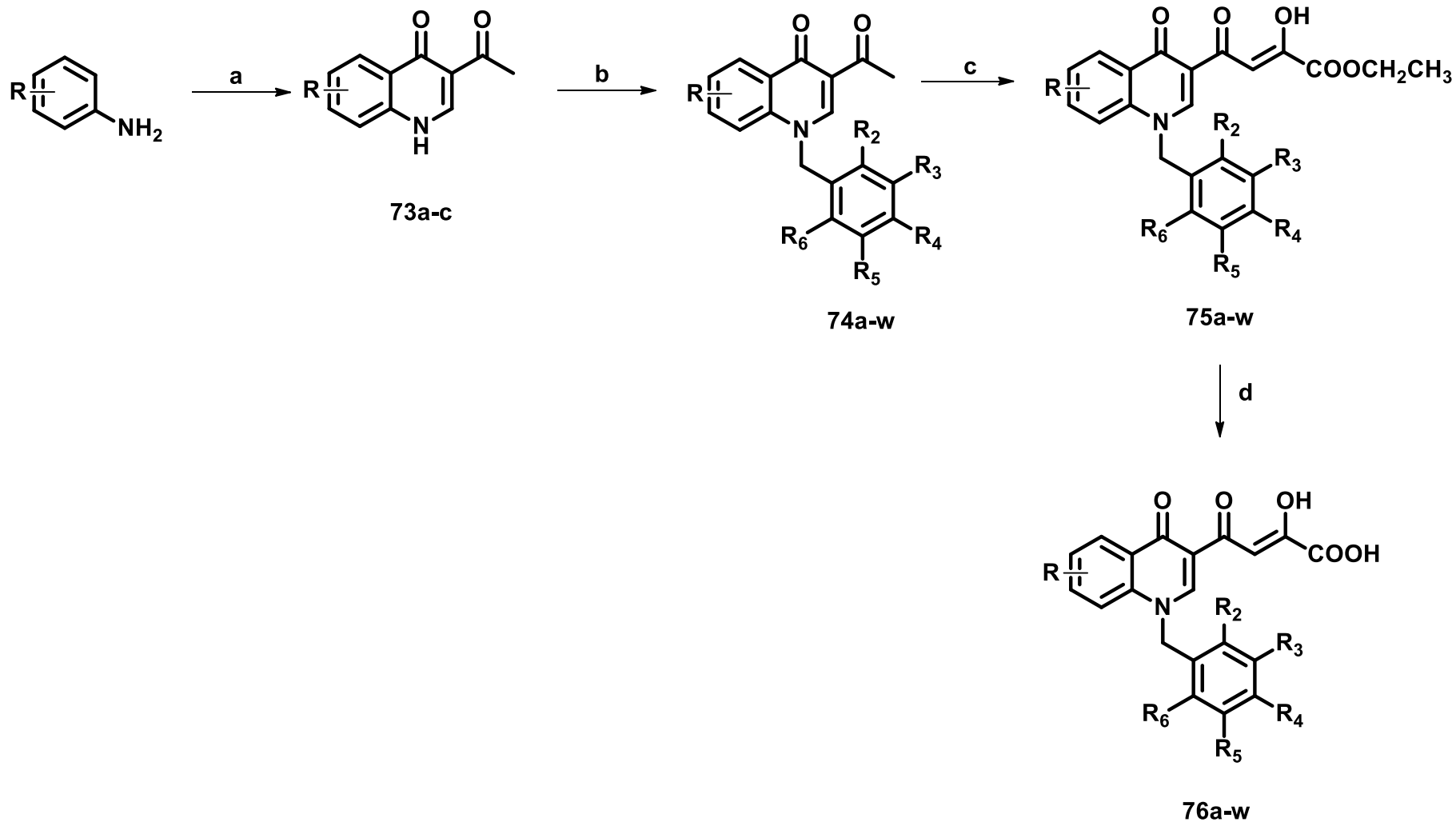


Role of N substituent

75a-w X=Et  
76a-w X=H

*J. Med. Chem.* 2015, 58, 4610-4623.

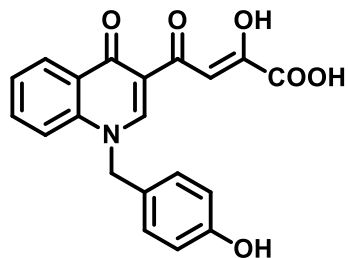
## Scheme 2. Synthetic Route to Quinolinonyl DKAs **75a-w** and **76a-w**.<sup>a</sup>



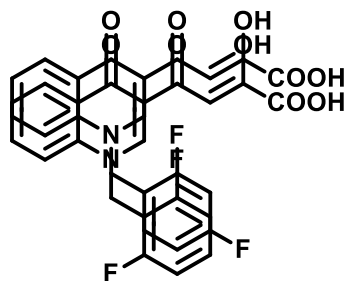
<sup>a</sup>Reagents and conditions: (i) ethyl orthoformate, ethyl acetoacetate, Dowtherm A, 95-254 °C, 8h, 52-58%; (ii) aryl bromide,  $K_2CO_3$ , DMF, 100°C, 50-75%; (iii) diethyl oxalate,  $C_2H_5ONa$ , THF, room temp, 10 min, 62-100%; (iv) 1 N NaOH, THF/MeOH, room temp, 40 min, 38-100%.

**Table 2.** Cytotoxicity, Antiviral, Anti-IN, anti-RNase H Activities of Compounds

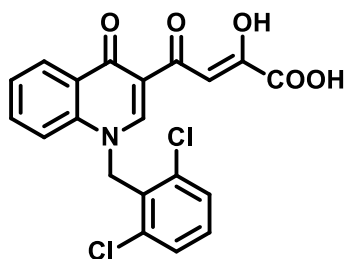
**75a-w and 76a-w.**



**76g**



**76j**

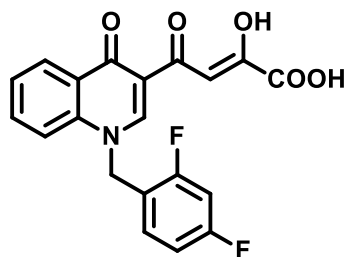


**76p**

Cpd	R	R <sub>2</sub>	R <sub>3</sub>	R <sub>4</sub>	R <sub>5</sub>	R <sub>6</sub>	X	3'-P	ST	IN (μM)	RNase H % in. <sup>b</sup>	IC <sub>50</sub> (μM)	EC <sub>50</sub> (μM) <sup>c</sup>	CC <sub>50</sub> (μM) <sup>d</sup>	SI <sup>e</sup>
75a	-	H	H	H	H	H	H	Et	>1000	0.70	-3.3	nd <sup>f</sup>	1	>50	50
75b	-	F	H	H	H	H	H	Et	125	0.28	2.8	nd	1.5	>50	>33.4
75c	-	OCH <sub>3</sub>	H	H	H	H	H	Et	>333	1.4	11.4	nd	2.6	>50	>19.2
75d	-	H	F	H	H	H	H	Et	>12.3	4.9	-9.4	nd	1.7	>50	>29.4
75e	-	H	OCH <sub>3</sub>	H	H	H	H	Et	>333	16	4.9	nd	8.5	44	5.2
75f	-	H	H	Cl	H	H	H	Et	>37	>37	16.1	nd	>50	nd	
75j	-	F	H	F	H	H	H	Et		2.2	3	nd	0.58	>50	>86.2
75k	-	F	H	H	F	H	H	Et		3.7	30	nd	>50	nd	
75l	-	F	H	H	H	F	Et	>12.3	0.25	4.1	nd	<0.2	>50	>250	
75m	-	H	F	F	H	H	Et		5.5	24	nd	9.8	>50	5.1	
75n	-	H	F	H	F	H	Et		11	24	nd	32.4	>50	>1.5	
75o	-	Cl	H	Cl	H	H	Et		>111	51	>50	>50	nd		
75p	-	Cl	H	H	H	Cl	Et		32	55.0	>50	30.2	>50	>1.7	
75q	-	CH <sub>3</sub>	H	CH <sub>3</sub>	H	H	Et		>111	33	>50	>50	nd		
75r	-	H	CH <sub>3</sub>	H	CH <sub>3</sub>	H	Et		1.3	21	nd	>50	nd		
75s	-	F	Cl	H	H	H	Et	1.08	1.08	21	nd	10	>50	>5	
76a	-	H	H	H	H	H	H	4.0	0.034	9.6	nd	15.5	nd		
76b	-	F	H	H	H	H	H	1.2	0.016	45.1	>50	2.6	>50	>19.2	
76c	-	OCH <sub>3</sub>	H	H	H	H	H	>4.1	0.038	45.2	16.3 ± 0.5	9.3	>50	>5.4	
76d	-	H	F	H	H	H	H	4.6	0.015	2.4	nd	28.2	>50	>1.8	
76e	-	H	OCH <sub>3</sub>	H	H	H	H	>4.1	0.14	1.9	nd	>50	nd		
76f	-	H	H	Cl	H	H	H	22	0.54	56.2	>50	0.87	>50	>57.5	
76g	-	H	H	OH	H	H	H	>37	0.45	44.4	9.5 ± 0.4	>50	nd		
76i	-	H	H	NO <sub>2</sub>	H	H	H	27	0.64	42.4	47.0 ± 1.5	>50	nd		
76j	-	F	H	F	H	H	H		0.010	46	35.9 ± 0.8	13.8	>50	>3.6	
76k	-	F	H	H	F	H	H		3.2	37	>50	>50	nd		
76l	-	F	H	H	H	F	H	0.7	0.019	57.9	10.8 ± 0.4	8.1	>50	>6.2	
76m	-	H	F	F	H	H	H		0.11	44	>50	16.2	>50	>3.1	
76n	-	H	F	H	F	H	H		0.22	30	>50	>50	nd		
76o	-	Cl	H	Cl	H	H	H		2.3	68	44.7 ± 2.0	>50	nd		
76p	-	Cl	H	H	H	Cl	H		0.27	86.3	10.0 ± 0.3	>50	nd		
76q	-	CH <sub>3</sub>	H	CH <sub>3</sub>	H	H	H		7.0	52	19.6 ± 0.6	>50	nd		
76r	-	H	CH <sub>3</sub>	H	CH <sub>3</sub>	H	H			0.05	47	37.8 ± 0.9	>50	nd	
76s	-	F	Cl	H	H	H	H	1.75	0.018	12	nd	23.4	>50	>2.1	
RAL (60)								12.8 ± 6 <sup>g</sup>	0.087	nd	>100	0.0236	>50	>2118	
ELV (61)								8.1 ± 4.2 <sup>g</sup>	0.028	nd	91 ± 8	0.0142	>50	>3521	

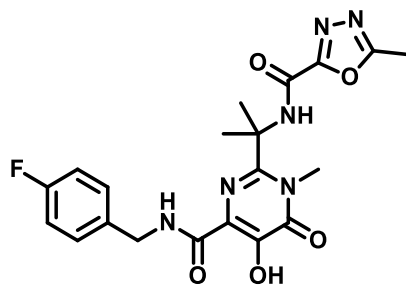
<sup>a</sup> Inhibitory concentration 50% (μM) determined from dose response curves. <sup>b</sup> Percentage of inhibition determined at compound concentration of 10 μM. <sup>c</sup> Effective concentration 50% (μM). <sup>d</sup> Cytotoxic concentration 50% (μM). <sup>e</sup> Selectivity index (CC<sub>50</sub>/EC<sub>50</sub>). <sup>f</sup> nd: not determined; <sup>g</sup> Reference 155

# Binding mode of compound 76j within the HIV-1 IN/DNA model



76j

Cmpd	IN IC <sub>50</sub> (μM)		RNase-H		Antiviral activity and cytotoxicity		
	ST	3'-P	IC <sub>50</sub> (μM)	%in. at 10μM	EC <sub>50</sub> (μM)	CC <sub>50</sub> (μM)	SI
76j	0.010	-	35.9± 0.8	46	13.8	>50	>3.6



RAL (60)

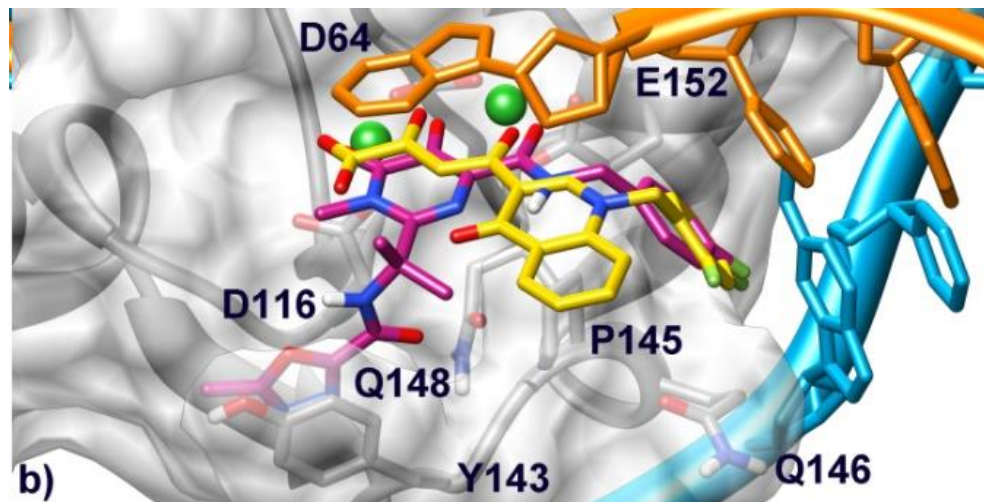
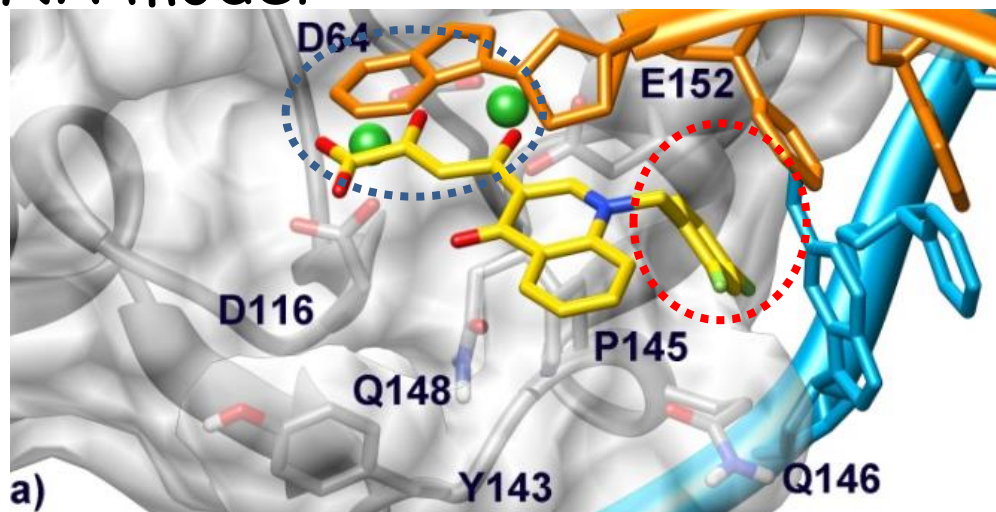
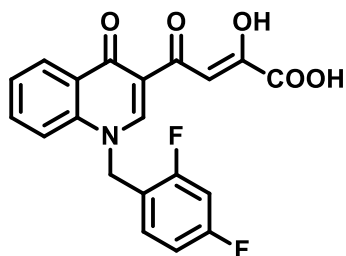


**Figure.** a) Binding mode of compound 76j (yellow) within the HIV-1 IN/DNA model. Catalytic core domain is depicted as transparent light gray surface and ribbons. Amino acid side chains important for the ligand binding are represented as sticks. The non-transferred (cyan) and reactive (orange) viral DNA strands are shown as ribbon and sticks. Mg<sup>2+</sup> metal ions are represented as green spheres. b) Overlay of compound 76j and RAL (magenta) in the IN binding pocket

# Binding mode of 76j in the HIV-1 RNase H active site.



76j

Cpd	IN IC <sub>50</sub> (μM)		RNase-H		Antiviral activity and cytotoxicity		
	ST	3'-P	IC <sub>50</sub> (μM)	%in. at 10μM	EC <sub>50</sub> (μM)	CC <sub>50</sub> (μM)	SI
76j	0.010	-	35.9± 0.8	46	13.8	>50	>3.6

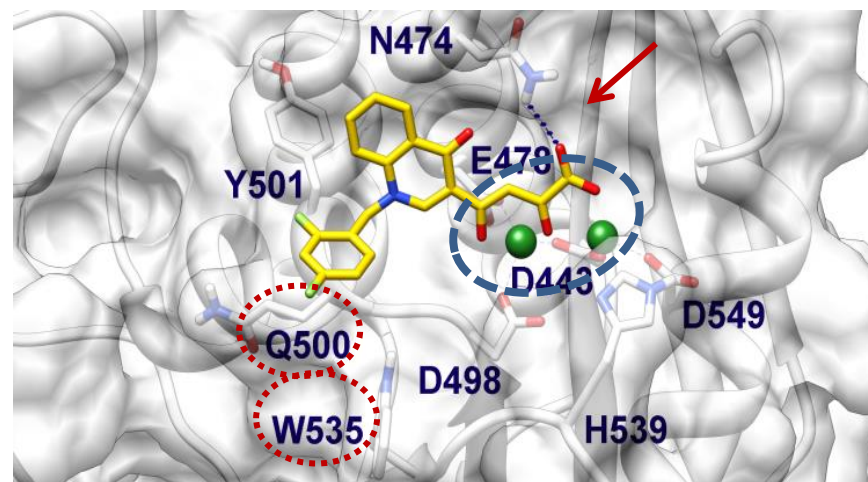
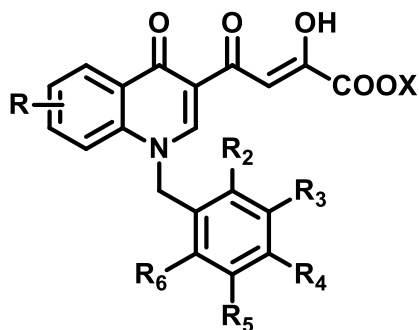


**Figure.** Binding mode of compound 76j (yellow) within the HIV-1 RNase H active site. Catalytic core domain is shown as transparent white surface and ribbons. Amino acid side chains important for the ligand binding are represented as sticks. Mg<sup>2+</sup> metal ions are depicted as green spheres.

*J. Med. Chem.* **2015**, *58*, 4610-4623.

# Conclusions 2

- Removal of the second DKA branch that directed the activity against 3'-P,
- Removal of the amino group in position 7 of quinolinone ring that addressed the activity on both IN and RNase H.
- Fine-tuning of the substituents on the benzyl group in 1 position of the quinolinone, that addressed the activity against IN ST, making secondary the activity against RNase H.



75a-w X=Et  
76a-w X=H

- The synthesized derivatives were tested in both enzyme- and cell-based assays as anti-HIV-1 agents and are able to selectively inhibit IN and only marginally the RNase H.

## Future studies:

- improve the activity of these compounds against HIV infected cells. Indeed the potency in cell-based assays was lower if compared to the enzymatic activity, suggesting that the acid derivatives are less prone to cell membrane penetration.

# Aim 3

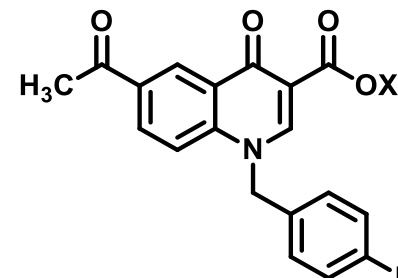
DKAs limits

- high metabolic turnover
- poor membrane penetration

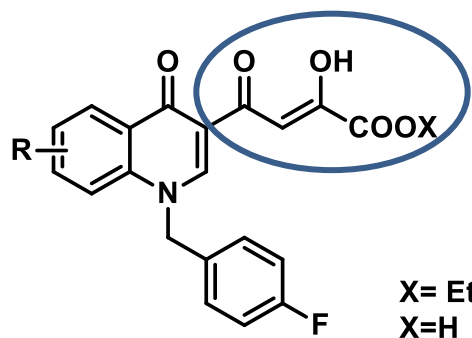


lower *in vivo* activity

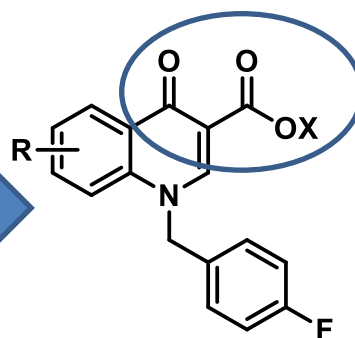
New Approach



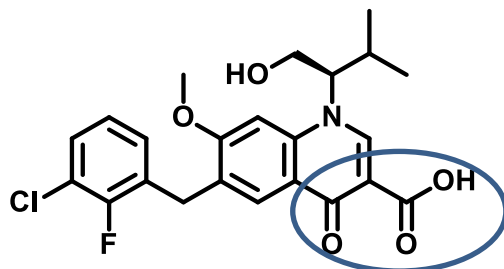
RDS 1599 (80) X=Et  
RDS 1600 (81) X=H



X= Et  
X=H



X=Et  
X=H



61

	IN		RNase-H	Antiviral activity and cytotoxicity	
	3'-P	ST		HIV-1 EC <sub>50</sub> (μM) <sup>c</sup>	CC <sub>50</sub> (μM) <sup>d</sup>
	IC <sub>50</sub> (μM) <sup>a</sup>		IC <sub>50</sub> (μM) <sup>b</sup>		
RDS 1599	>1000	>1000	11.0	0.5	22
RDS 1600	>1000	>1000	16	0.29	25

<sup>a</sup> Inhibitory concentration 50% (μM) determined from dose response curves. <sup>b</sup> Inhibitory concentration 50% (μM). <sup>c</sup> Effective concentration 50%. <sup>d</sup> Cytotoxic concentration 50% (μM).

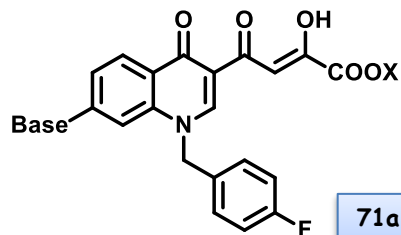
# Conclusions 3

advantage

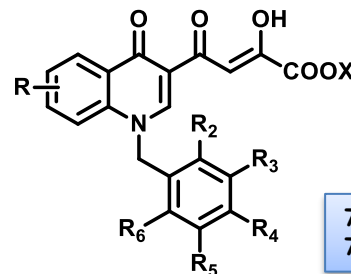


limits

- Highly Active Anti-Retroviral Therapy (HAART)
- New anti-HIV agents are still needed.
- The use of dual-action drugs is a novel and highly promising approach: **71a-g,i** and **72a-g,i**; **75a-w** and **76a-w**. These compounds were nanomolar INSTIs and also exhibited low micromolar RNase H inhibition and antiviral properties.

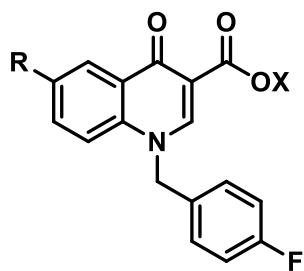


71a-g,i X=Et  
72a-g,i X=H

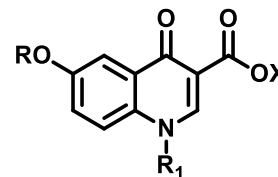


75a-w X=Et  
76a-w X=H

- About identification of new viral target: RNase H function is an attractive drug target, it is essential for retroviral replication and none RNase H inhibitor has been approved yet. New series **84a-g**, **92h-m**, **85a-g** and **93h-m** was designed inspiring by the experimental results of Elvitegravir. Further informations will be soon available since the molecular modeling studies and the cell-based assays are ongoing.



84a-g X=Et  
85a-g X=H



92h-m X=Et  
93h-m X=H

# Acknowledgements

Prof. R. Di Santo  
Prof. R. Costi



Prof. Y. Pommier  
Dr. C. Marchand  
Prof S. Le Grice

**DIPARTIMENTO DI CHIMICA  
E TECNOLOGIE DEL FARMACO**



Prof. E. Tramontano  
Dr.ssa A. Corona



Prof. E. Novellino  
Dr. S. Cosconati

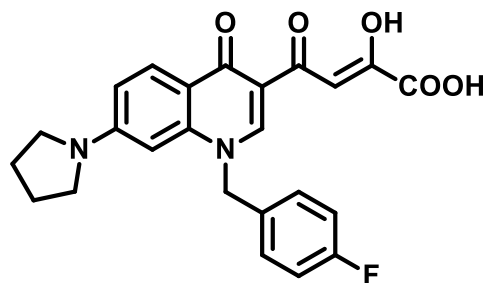


Prof. P. Van der Veken  
Dr. Y. Adriaenssens

University of Antwerp

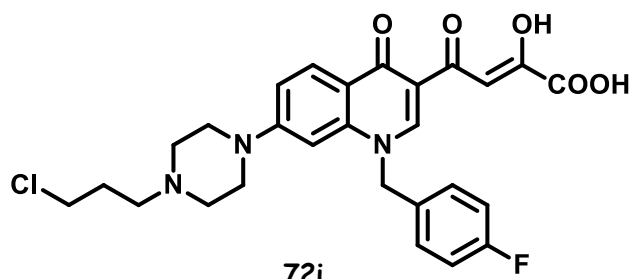
**THANKS FOR  
YOUR KIND  
ATTENTION**

# Binding Mode of 72i within HIV-1 IN/DNA model.



**67b**

Cmpd	IN IC <sub>50</sub> (μM)		RNase-H IC <sub>50</sub> (%)	
	ST	3'-P	(μM)	in. at 10 μM
67b	0.028	14.9	5.1	71



**72i**

Cmpd	IN IC <sub>50</sub> (μM)		RNase-H IC <sub>50</sub> (%)	
	ST	3'-P	(μM)	in. at 10 μM
72i	0.05±0.01	4.6±0.5	5.7±0.1	78

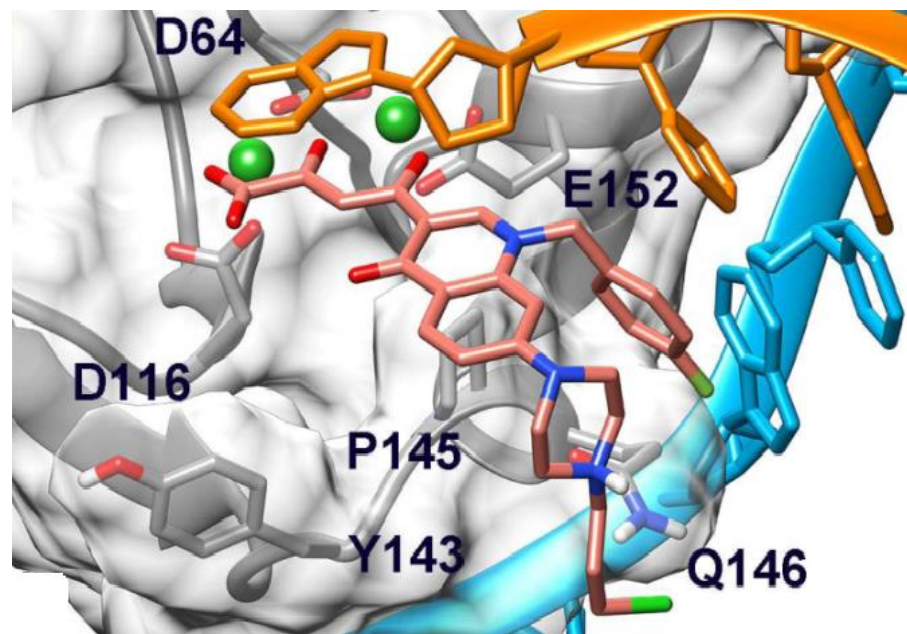
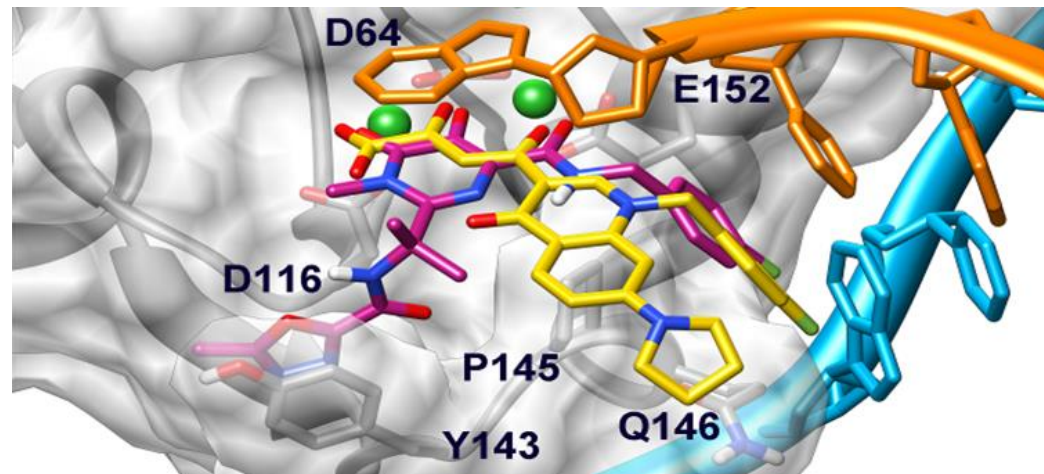
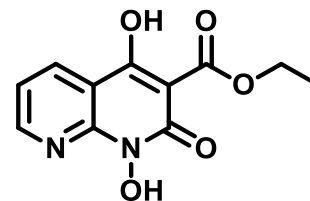
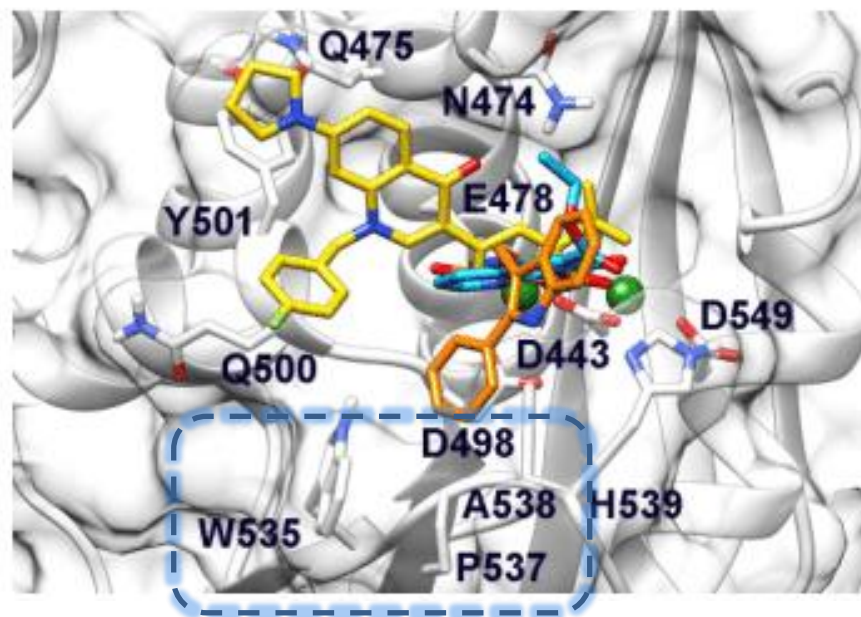
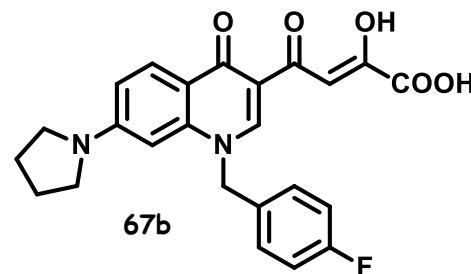


**Figure.** Overlay of compound **67b** and Raltegravir (magenta) in the IN binding pocket and binding modes of compound **72i** (pink sticks) within the HIV-1 IN/DNA model. The CCD is depicted as transparent light gray surface and ribbons. Amino acid side chains involved in ligand binding are represented as sticks. The non-cleaved (cyan) and processed (orange) viral DNA strands are shown as ribbon and sticks. Mg<sup>2+</sup> metal ions are represented as green spheres.

# Comparison between the binding modes of **67b** and a naphthyridinone and a pyrimidinol carboxylic acid.

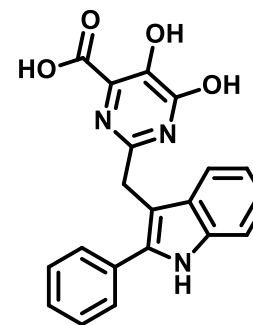


$IC_{50} \sim 0.11 \mu M$



**67b**

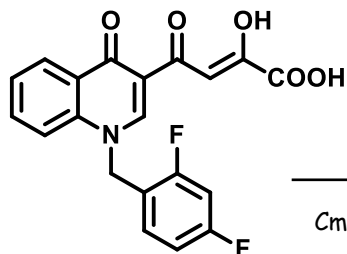
Cmpd	IN		RNase-H	
	ST	3'-P	$IC_{50}$ ( $\mu M$ )	% in. at $10 \mu M$
<b>67b</b>	0.028	14.9	5.1	71



$IC_{50} 0.23 \pm 0.01 \mu M$

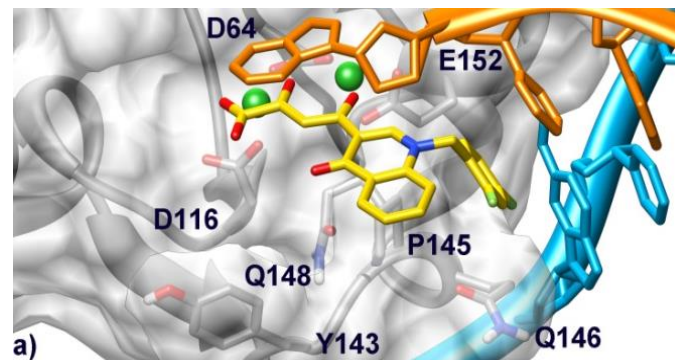
**Figure.** Comparison between the binding modes of **67b** (yellow) and a naphthyridinone and a pyrimidinol carboxylic acid co-crystallized with the HIV-1 RT enzyme at the RNase H active site (PDB codes 3LP01 and 3QIP2). The active site is shown as transparent white surface and ribbons. Amino acid side chains important for ligand binding are represented as sticks.  $Mg^{2+}$  metal ions are depicted as green spheres.

# Binding mode of 75j and 76j in the HIV-1 RNase H active site and IN

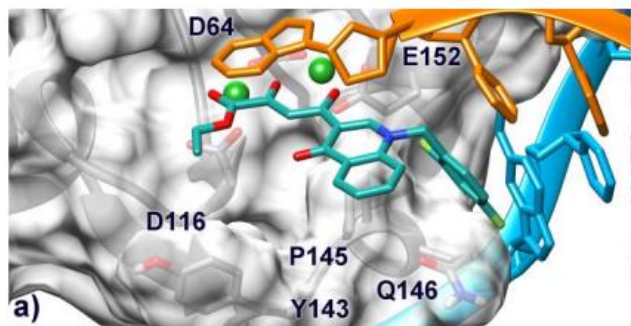


76j

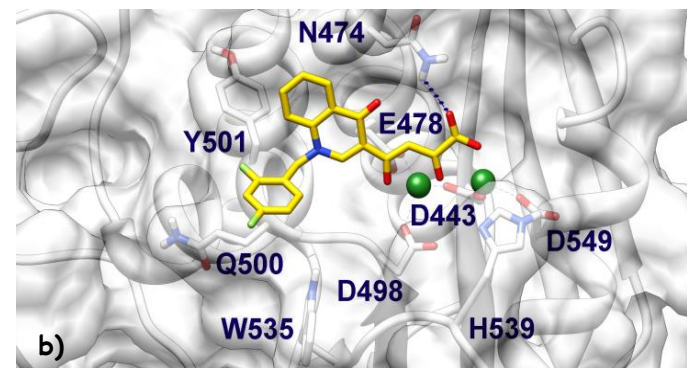
Cmpd	IN IC <sub>50</sub> (μM)		RNase-H		Antiviral activity and cytotoxicity		
	ST	3'- P	IC <sub>50</sub> (μM)	%in. at 10 μM	EC <sub>50</sub> (μM)	CC <sub>50</sub> (μM)	SI
76j	0.010	-	35.9± 0.8	46	13.8	>50	>3.6



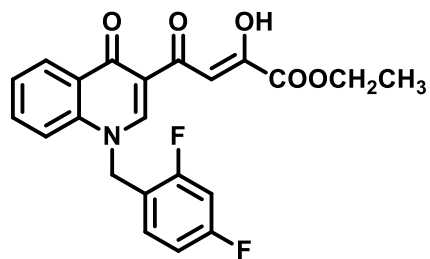
a)



a)

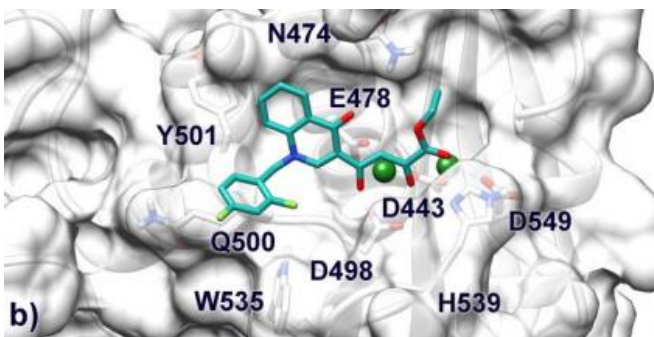


b)



75j

Cmpd	IN IC <sub>50</sub> (μM)		RNase-H		Antiviral activity and cytotoxicity		
	ST	3'- P	IC <sub>50</sub> (μM)	%in. at 10 μM	EC <sub>50</sub> (μM)	CC <sub>50</sub> (μM)	SI
75j	2.2	-	-	31	0-58	>50	>86.2



b)